STEM CELLS®

STEM CELL TECHNOLOGY: EPIGENETICS, GENOMICS, PROTEOMICS, AND METABONOMICS

Treatment of Human Mesenchymal Stem Cells with Angiotensin Receptor Blocker Improved Efficiency of Cardiomyogenic Transdifferentiation and Improved Cardiac Function via Angiogenesis

YOHEI NUMASAWA,[a] TAKEHIRO KIMURA,[a] SHUNICHIRO MIYOSHI,[a] NOBUHIRO NISHIYAMA,[a] NAOKO HIDA,[a] HIROKO TSUJI,[a] HIKARU TSURUTA,[a] KAORU SEGAWA,[b] SATOSHI OGAWA,[a] AKIHIRO UMEZAWA[c]

[a]Department of Cardiology and [b]Department of Microbiology and Immunology, Keio University School of Medicine, Tokyo, Japan, [c]Department of Reproductive Biology and Pathology, National Research Institute for Child Health and Development, Tokyo, Japan

Key Words. Angiotensin • Bone marrow stromal cells • Transdifferentiation • Stem cell transplantation

ABSTRACT

To improve the modest efficacy of mesenchymal stem cell (MSC) transplantation, the treatment of human MSCs with angiotensin receptor blockers (ARBs) was investigated. MSCs were cultured with or without the medium containing 3 μmol/l of ARBs before cardiomyogenic induction. After cardiomyogenic induction in vitro, cardiomyogenic transdifferentiation efficiency (CTE) was calculated by immunocytochemistry using anticardiac troponin-I antibody. In the nude rat chronic myocardial infarction model, we injected MSCs pretreated with candesartan (A-BM; $n = 18$) or injected MSCs without pretreatment of candesartan (BM; $n = 25$), each having survived for 2 weeks. The left ventricular function, as measured by echocardiogram, was compared with cardiomyogenic transdifferentiation in vivo, as determined by immunohistochemistry. Pretreatment with ARBs significantly increased the CTE in vitro (10.1 ± 0.8 $n = 12$ vs. 4.6 ± 0.3% $n = 25$, $p < .05$). Transplantation of candesartan-pretreated MSCs significantly improved the change in left ventricular ejection fraction (BM; −7.2 ± 2.0 vs. A-BM; 3.3 ± 2.3%). Immunohistochemistry revealed significant improvement of cardiomyogenic transdifferentiation in A-BM in vivo (BM; 0 ± 0 vs. A-BM; 0.014 ± 0.006%). Transplantation of ARB-pretreated MSCs significantly improved cardiac function and can be a promising cardiac stem cell source from which to expect cardiomyogenesis. STEM CELLS *2011;29:1405–1414*

Disclosure of potential conflicts of interest is found at the end of this article.

INTRODUCTION

Regeneration therapies have attracted a great deal of medical attention. Various cellular resources such as embryonic stem cells [1], mesenchymal stem cells (MSCs) [2], mononuclear cells [3, 4], and endothelial progenitor cells (EPCs) [5] have been candidates for the regeneration therapies. The majority of cells derived from bone marrow (BM) consist of blood cells in various stages of differentiation; however, BM also contains, hematopoietic stem cells, EPCs, and MSCs. MSCs have characteristics of replication competence and multipotency [2, 6–8], as reported in numerous studies of MSCs.

Mesenchymal cells are classified as somatic stem cells and exist in BM stroma, dermis, skeletal muscle, uterine endometrial gland [9], umbilical cord blood [7, 10], placenta [11], amniotic membrane [6], etc. They are known to be capable of transdifferentiating into bone, cartilage, skeletal muscles, fats, ligaments, vascular endothelium, smooth muscle, and cardiomyocytes. Among the various mesenchymal cell sources, BM-derived MSCs (BM-MSCs) can be used in an autologous manner; therefore, there are no immunological problems in transplantations. However, in terms of cardiomyogenic transdifferentiation, the efficiency of human BM-MSCs is extremely low [8] in vitro, and efficiency of human BM-MSC transplantation is modest in in vivo [12, 13] and in clinical trials [14, 15]. The limited effect in clinical trials may be due to low angiogenic and paracrine effect of human BM-MSCs, low cardioprotective effect on host myocardium, and partially due to low cardiomyogenic transdifferentiation efficiency (CTE) [8]. We have previously shown that human mesenchymal cells derived from younger populations, that is,

Author contributions: Y.N., T.K., N.N., H. Tsuji, H. Tsuruta, and K.S.: conception and design, collection and assembly of data, final approval of manuscript; S.M.: conception and design, administrative support, collection and assembly of data, data analysis and interpretation, manuscript writing, final approval of manuscript; N.H.: conception and design, collection and assembly of data; S.O.: financial support, administrative support, final approval of manuscript; A.U.: financial support, administrative support, final approval of manuscript. Y.N. and T.K. contributed equally to this article.

Correspondence: Shunichiro Miyoshi, M.D., Ph.D., Keio University School of Medicine, 35-Shinanomachi, Shinjuku-ku, Tokyo 160-8582, Japan. Telephone: 81-3-3353-1211, ext. 61421; Fax: 81-3-5363-3875; e-mail: smiyoshi@cpnet.med.keio.ac.jp Received March 8, 2011; accepted for publication June 30, 2011; first published online in STEM CELLS *EXPRESS* July 13, 2011. 1066-5099/2009/$30.00/0 doi: 10.1002/stem.691

endometrial gland [9], umbilical cord blood [10], placenta [11], and amniotic membrane [6] have a high CTE and a beneficial effect on cardiac function. Therefore, we hypothesized that mesenchymal cells obtained from younger populations might have a better effect on regeneration therapies. As angiotensin receptor blocker (ARB) was known to have the potential to play a role in the anti-aging effect, we postulated that ARB might improve the efficacy of BM-MSCs on cardiac stem cell therapy.

Stimulation of angiotensin receptors is known to be related to adipogenic transdifferentiation of human BM-MSCs [16]. In the brain ischemic reperfusion model, BM-MSC transplantation significantly reduced the brain infarction area via improvement of brain blood flow and reduction of oxidative stress [17]. The effect of BM-MSC transplantation was abolished by knocking out the angiotensin-II (AT) receptor type-II (AT2R). On the other hand, this effect was restored by pretreatment with ARB for BM-MSCs in the culture. These facts suggest that ARB and stimulation of AT receptor may play a significant role in causing the angiogenesic effect of BM-MSC transplantation. Therefore, in this study, we investigated the effect of ARB on CTE of human BM-MSCs in vitro and in vivo, and efficacy of BM-MSC transplantation on cardiac function in the myocardial infarction (MI) model in vivo.

Materials and Methods

BM-Derived MSCs

Yub623 (RIKEN Cell bank, Cell No. HMS0017, Tokyo, Japan) cells were used as BM-MSCs in this study. Yub623 is a fibroblast-like shaped human MSC (hMSC) derived from neonatal human BM from a finger of patients with polydactyly. Cells were cultured in high-glucose supplemented Dulbecco's modified Eagle's medium containing 10% human serum.

Cardiomyogenic Induction and Chemical Agents

The method of cardiomyogenic induction in vitro was described previously (Supporting Information Material and Method-1) [6, 8–11]. In short, enhanced green fluorescent protein (EGFP) labeled BM-MSCs were cocultured with murine cardiomyocytes. In this system, the incidence of cell fusion was approximately 0.3% and the evidence of cell fusion-independent cardiomyogenesis was extensively shown in the previous studies [6, 8–11, 18, 19]. BM-MSCs were preincubated with chemical agent-containing medium for 2 weeks before coculture and/or cultured with chemical agent-containing medium after coculture. In this study, we used 3 μmol/l of telmisartan (tel), candesartan (cnd), losartan (los), olmesartan (olm), and valsartan (val) as an AT receptor blocker (ARB), 3 μmol/l of PD123319 (pd) as a specific AT type-I blocker; enalaprilat (ena) and captopril (cap) as an angiotensin converting enzyme (ACE) inhibitor; 3 μmol/l of aliskiren (ali) as a direct rennin inhibitor; 1 μmol/l of AT; and 10 μmol/l of GW9662 (gw) as a peroxisome proliferators-activated receptor-γ (PPAR-γ) blocker. Evaluation of efficiency of cardiomyogenic transdifferentiation was described previously [6, 10, 11]. In short, cocultivated BM-MSCs were enzymatically isolated, a smear sample was made, and then immunocytochemistry using mouse monoclonal antibody against anticardiac troponin-I (Trop-I, #4T21 Hytest, Euro, Finland) antibody was performed (described later). Isolated cells (spherical shape), in which Trop-I colocalized with EGFP at the cytoplasm were considered as Trop-I/EGFP double positive cells. The CTE was defined as the incidence of Trop-I/EGFP double positive cells in EGFP-positive BM-MSCs. The incidence of cell fusion was not affected by ARB treatment (0.30% to 0.39%) in this study.

Immunocytochemistry and Immunohistochemistry

A laser confocal microscope (FV1000, Olympus, Tokyo, Japan) was used. As described previously [6, 8–11, 18, 19], samples were stained with Trop-I with mouse monoclonal antibody (sigma) and rabbit polyclonal anti-connexin 43 antibody (sigma) diluted 1:300 overnight at 4°C, then stained with TRITC-conjugated anti-mouse IgG antibody (Sigma) and Cy5-conjugated anti-rabbit IgG antibody (Chemicon) diluted 1:100, containing 4′-6-diamidino-2-phenylindole (Wako) at 1:300 for 30 minutes at 25–28°C.

Enzyme-Linked Immunosorbent Assay

Angiogenic humoral factors (angiogenin, angiotensin-2, epidermal growth factor [EGF], basic fibroblast growth factor, heparin-binding EGF-like growth factor, hepatocyte growth factor, phosphatidylinositol-glycan biosynthesis class F protein, and vascular endothelial growth factor) in culture medium supernatant (cultured with 10% serum-containing medium for 7 days) were measured by enzyme-linked immunosorbent assay [19]. The assay was performed with Quantibody Human Angiogenesis Array I kit (RayBiotec, Inc. GA) and was conducted according to manufacturer recommended protocol.

Gene Chip Analysis

Human genome-wide gene expression was examined with the Human Genome U133A Probe array (Affymetrix), which contains the oligonucleotide probe set for approximately 23,000 full-length genes and expressed sequence tags as described previously [11, 20].

Transplantation of ARB-Pretreated BM-MSCs in MI Model In Vivo

MI was induced in the open chests of anesthetized female F344 nude rats (Clea Japan, Inc., 6 weeks of age) as described previously [6, 9, 19]. Two weeks after MI, 1–2 $\times$ 10^6 of EGFP-labeled BM-MSCs were injected into the myocardium at the border zone of the MI. Two weeks after the first operation, rats with MI were randomized in a blind study of the following groups: the sham operated group (Sham), the (CNT), the CNT with plain BM-MSC transplanted group (BM), and the MI+candesartan-pretreated BM-MSC transplanted group (A-BM). After cellular transplantation, TCV-116 (stable form of candesartan; 0.5 mg/kg/day) was orally administered in some of the experiments (+A). Randomization occurred immediately before echocardiogram. Immediately before cell transplantation, two-dimensional and M-mode echocardiographic (8.5 MHz linear transducer; EnVisor C, Phillips Medical System, Andover, MA) images were obtained to assess left ventricular (LV) end-diastolic dimension and LV end-systolic dimension (LVESD) at the mid-papillary muscle level by a single blinded observer. Two weeks after the transplantation, a similar echocardiogram was performed again. LV percentage fractional shortening, thickness of anterior wall (AW), and thickness of posterior wall were calculated from five to six traces and averaged. LV pressure, brain natriuretic peptide (BNP), body weight, and heart weight (wet) were measured as described previously. Tissue samples were obtained by slicing along the short axis of the left ventricle, for every 1 mm of depth. After masson trichrom staining, the area of fibrosis was digitized from each slice, and then the percentage fibrosis volume in the LV myocardium was calculated as described previously [6, 19]. Immunohistochemical analysis was performed to observe CTE in vivo as described previously (Supporting Information Material and Method-2). Immunohistochemical analysis was performed using anti-rat CD34 antibody (1:200 R&D Systems; AF4117) to evaluate vascular density. Then, biotinylated goat immunoglobulins (Dako; E0466) were used as a second antibody, next, strept avidin biotin complex (ABC) complex/horseradish peroxidase (HRP) (Dako; K0377), and, finally, 3,3′-Diaminobenzidine substrate (Wako; K3183500) were used. The images were digitized and the percentage brown pixel area of the capillary vessels was counted in the peri-infarct normal zone (NZ) and the center of the MI

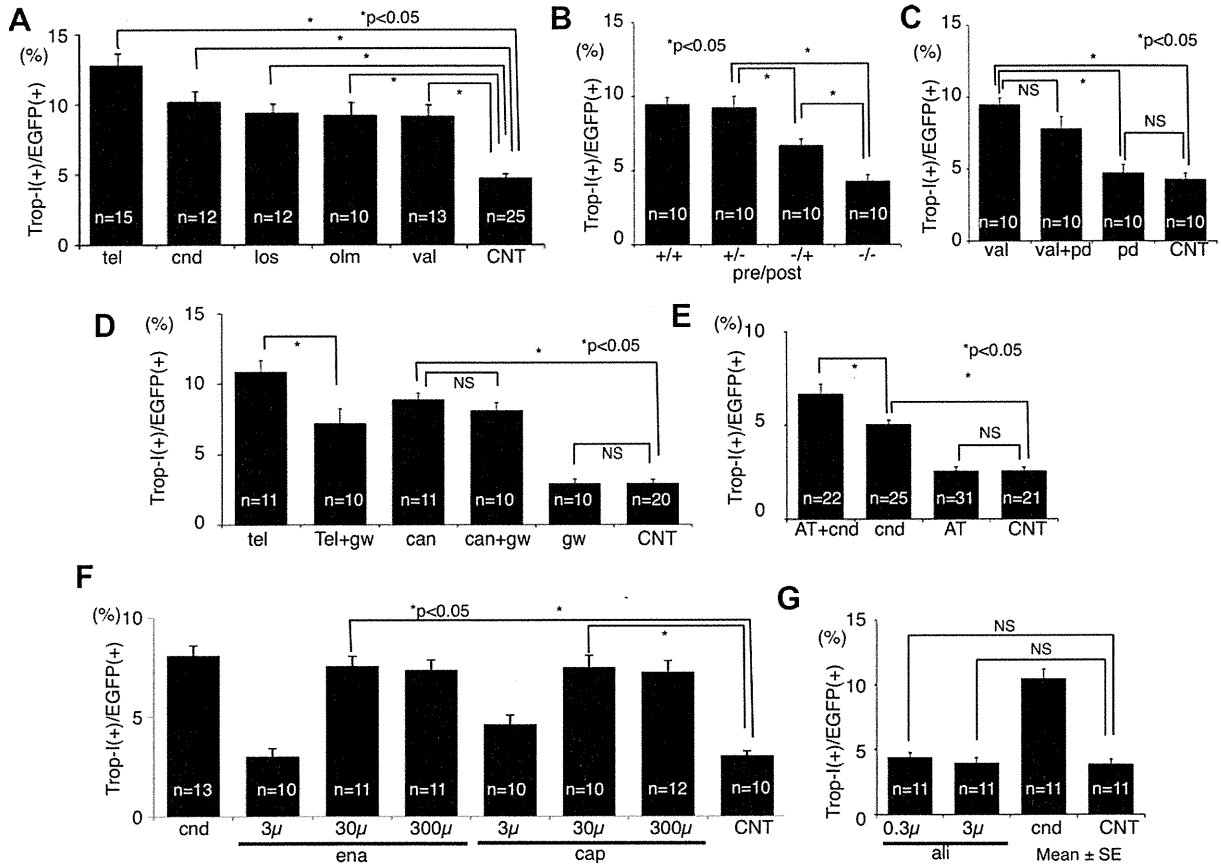

Figure 1. Improvement of cardiomyogenic transdifferentiation efficiency (CTE) of bone marrow-derived mesenchymal stem cells (BM-MSC) by blockade of renin-angiotensin system in vitro. The calculated rate of cardiac troponin-I positive cells in enhanced green fluorescent protein-positive cells are averaged and shown as CTE. **(A):** The effect of pretreatment with telmisartan (tel), candesartan (cnd), losartan (los), olmesartan (olm), and valsartan (val) on CTE of human BM-MSCs are shown. CNT denoted CTE of control MSCs. These ARBs increase CTE significantly. **(B):** Condition of pretreatment of val (before slash) and val treatment after induction (after slash) are shown in the bottom. Pretreatment of val significantly increased CTE and was essential for val-induced CTE increase. Val treatment after induction moderately increased CTE. **(C):** The effect of combination of val as a specific angiotensin-II (AT) receptor type-I (AT1R) blocker and PD123319 (pd) as a specific AT2R blocker to CTE is shown. The pd did not affect CTE. **(D):** The effect of GW9662 (gw) as a specific peroxisome proliferators-activated receptor-γ (PPAR-γ) blocker on tel-induced CTE increase and cnd-induced CTE increase are shown. The blockade of PPAR-γ partially blocked the tel-induced CTE increase and did not affect cnd-induced CTE increase. **(E):** The effect of additional application AT in the presence or in the absence of cnd is shown. AT alone did not affect CTE; however, AT significantly increased CTE in the presence of cnd. **(F):** Dose-response effect of pretreatment with enalaprilat (ena) and captoril (cap) as angiotensin converting enzyme inhibitors (ACEI). ACEI significantly improves CTE in a dose-dependent manner. **(G):** The effect of aliskiren (ali) as a renin inhibitor on CTE is shown. Ali did not affect CTE. *p<0.05. Abbreviations: ali, aliskiren; AT, angiotensin-II; cap, captoril; cnd, candesartan; CNT, control; EGFP, enhanced green fluorescent protein; ena, enalaprilat; gw, GW9662; los, losartan; olm, olmesartan; pd, PD123319; Tel, telmisartan; Trop-I, troponin-I; val, valsartan.

zone (MI) using a light microscope at 10× magnification. The areas in five high-power fields were calculated and averaged.

Statistical Analysis

All data are shown as mean value ± SE. The difference between mean values was determined with one-way analysis of variance (ANOVA) test or one-way repeated measures ANOVA test and Bonferroni post hoc test. Statistical significance was set at $p < .05$.

Results

Pretreatment with ARB Increased Efficiency of Cardiomyogenic Transdifferentiation Via AT2R

Administration of 3 μmol/l of popular ARBs (tel, can, los, olm, and val) did not cause any significant change in morphology of BM-MSCs (Supporting Information Fig. 1A, 1B), while improved CTE in vitro was observed (Fig. 1A and Supporting Information Fig. 1C–1P). In our pilot study, we tested dose-response effect of ARBs and confirmed that this effect was saturated at the concentration of 3 μmol/l (CTE at control, 0.03, 0.3, 3, and 30 μmol/l of cnd were 3.0 ± 0.3, 3.5 ± 0.2, 4.8 ± 0.3, 8.9 ± 0.4, and 8.1 ± 0.5%, respectively). Therefore, in this study, we selected 3 μmol/l as a default concentration of ARBs. To clarify the target of the ARBs, val was administrated only before the coculture or only after the coculture (Fig. 1B). Administration of val after the start of coculture (±) caused modest improvement of CTE; on the other hand, administration of val before the start of coculture (±) significantly increased CTE, suggesting that val modified the character of the BM-MSCs so as to be able to cause higher CTE. To determine whether the effect of the ARBs was mediated by AT receptor type-I (AT1R) or AT2R, we used val as AT1R specific blocker and pd as AT2R specific blocker (Fig. 1C). Administration of pd did not affect CTE, while val increased CTE significantly. Furthermore, CTE with both val and pd administered did not show an additional increase

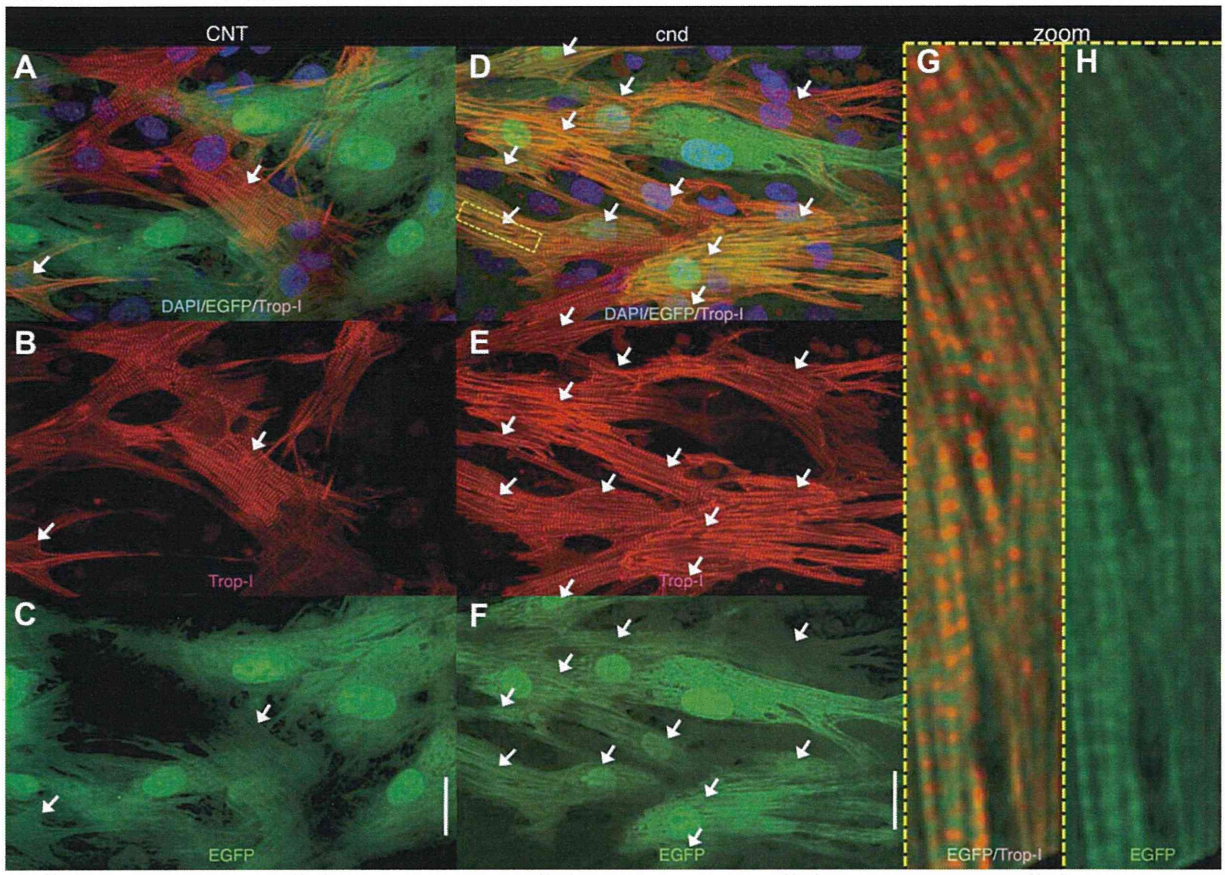

Figure 2. Confocal laser microscopic images of the immunocytochemical analysis of transdifferentiated cardiomyocytes. Confocal microscopic images of immunocytochemistry after cardiomyogenic induction using anti-cardiac troponin-I (red: Trop-I) revealed significant augmentation of enhanced green fluorescent protein (EGFP) (green)/Trop-I double positive cardiomyocytes (white arrow) by candesartan (cnd) (**D–F**) pretreatment, while EGFP/Trop-I double positive cells were rare in CNT (**A–C**). Area within the dotted yellow box is expanded and shown in (**G, H**). Clear striation staining pattern of Trop-I was observed in every EGFP-positive cell. The striating pattern of EGFP and Trop-I appeared in alternation, suggesting that the Trop-I was expressed in the EGFP-positive cells. Scale bar = 20 μm. Abbreviations: cnd, candesartan; CNT, control; DAPI, 4′-6-diamidino-2-phenylindole; EGFP, enhanced green fluorescent protein; Trop-I, troponin-I.

(rather, tended to show a statistically nonsignificant decrease). These data suggest that blockade of AT1R plays a pivotal role in ARB-dependent CTE increase. We have previously reported that PPAR-γ activator has an ability to increase CTE of BM-MSCs [19], and some of the ARBs, that is, tel, have a potential to activate the PPAR-γ. To clarify that the mechanism of ARB-induced CTE increase was mediated via PPAR-γ activation effect, we used gw as a specific blocker for PPAR-γ (Fig. 1D). The gw partially blocked tel-induced CTE increase; on the other hand, it did not block cnd-induced CTE increase. These data suggest that the effect of cnd on CTE was independent from PPAR-γ activation. In our previous study, the effect of pio was completely blocked by gw [19]; therefore, the gw-insensitive tel-induced CTE increase was caused by a PPAR-γ-independent mechanism. On the other hand, administration of AT did not affect CTE in the absence of ARB, while administration of AT significantly increased CTE in the presence of ARB (Fig. 1E). These data suggest both blockade of AT1R and stimulation of AT2R increase CTE. The increase in CTE was also observed by administration of ACE inhibitors ena or cap (Fig. 1F), suggesting the source of AT in this system is autocrine of angiotensin-I from BM-MSCs and local ACE activity. Furthermore, the effect was not blocked by the specific renin blocker, ali (Fig. 1G); therefore, angiotensinogen does not play a role as an AT source in this system, but a local angiotensin-generating system may play a role in this phenomenon.

The Effect of ARB-Treated BM-MSC Transplantation on Cardiac Function In Vivo

The BM-MSCs were transplanted into the hearts of nude rats with chronic MI, in vivo, and the effect on cardiac function was examined. Representative M-mode echocardiographic images at 2 weeks after transplantation are shown (Fig. 2A). In the CNT group, akinesis and thinning of AW are observed. There were no marked changes in the BM group, while in A-BM group, the motion of AW markedly improved. The same trend was also observed in the ARB orally administered group (+A group). The changes in echocardiographic parameters between the immediately before the transplantation group (post MI 2 weeks) and the 2 weeks after transplantation group (post MI 4 weeks) are compared (Fig. 3). Changes in LV ejection fraction (ΔLVEF) were decreased as a function of time, even 2 weeks after the MI, which may be due to LV remodeling. The transplantation of plain BM-MSCs (BM) did not have an effect on ΔLVEF; on the other hand, candesartan-pretreated BM-MSCs (A-BM) significantly improved ΔLVEF. The degree of improvement was marked when candesartan was orally administered (A-BM-A). Change in end-diastolic diameter of LV (ΔLVEDD) did not differ among the

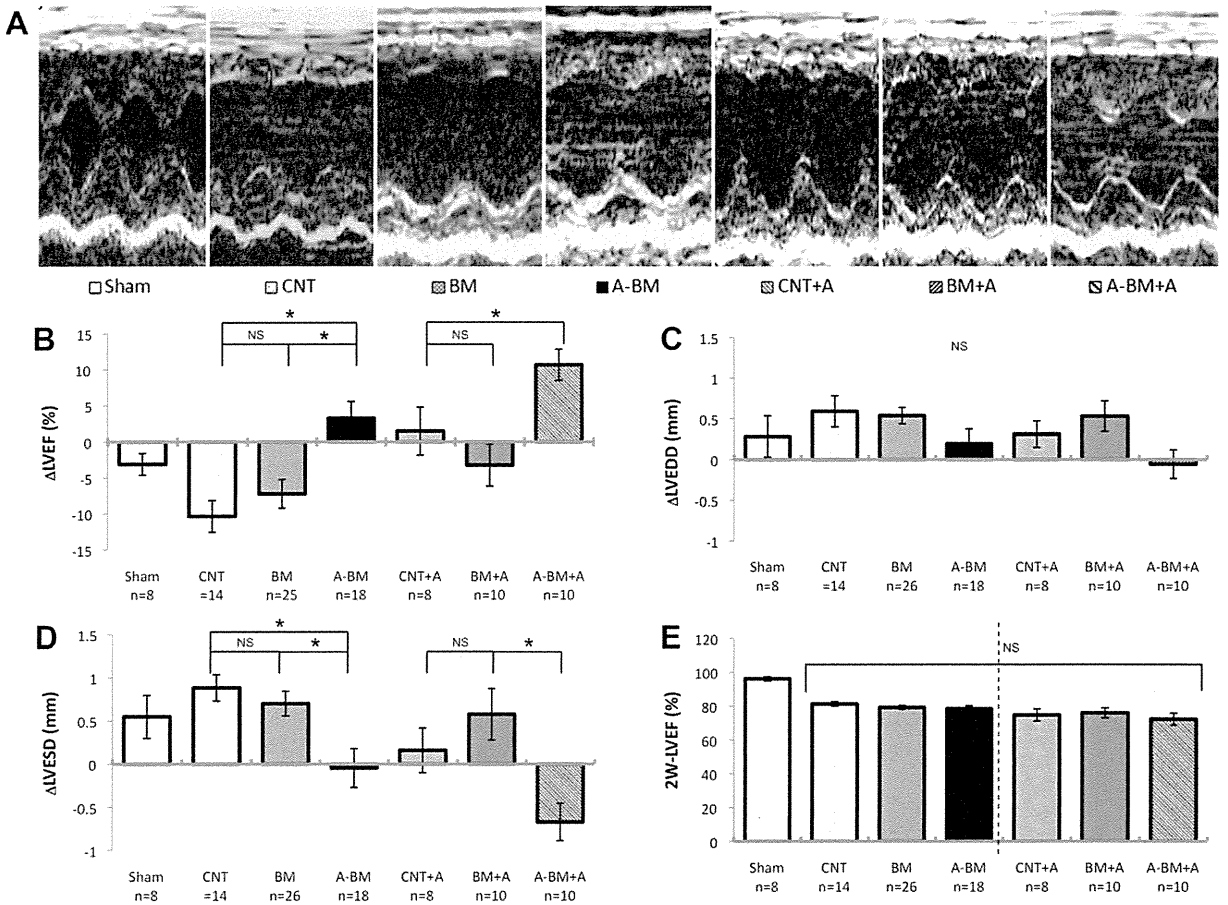

Figure 3. Effect of candesartan-pretreated bone marrow-derived mesenchymal stem cell (BM-MSC) transplantation and/or oral administration of candesartan on echocardiographic parameters in vivo. **(A):** Representative trace of M-mode echocardiogram from Sham-operated nude rats, control myocardial infarction (MI) (CNT), MI with BM-MSCs transplantation (BM), candesartan-pretreated BM (A-BM), and oral administration of candesartan after the transplantation (CNT+A, BM+A, A-BM+A) is shown. Changes in left ventricular ejection fraction (LVEF) from 2 to 4 weeks **(B**; ΔLVEF), LV end-diastolic dimension **(C**; ΔLVEDD), and LV end-systolic dimension **(D**; ΔLVESD) are averaged and shown. **(E):** Calculated LVEF from each group at 2 weeks after first operation are shown. There was no statistical significance; however, the degree of percentage EF tends to be worse in the oral administration series (right columns separated by dotted bar). Candesartan-pretreated BM significantly improved LVESD, consequently improved LVEF. *$p<0.05$. Abbreviations: BM, bone marrow; CNT, control; LVEDD, left ventricular end-diastolic dimension; LVEF, left ventricular ejection fraction; LVESD, left ventricular end-systolic dimension.

groups; on the other hand, change in LVESD (ΔLVESD) was significantly improved in A-BM group (vs. BM group) and A-BM+A group (vs. BM+A group), suggesting transplantation of candesartan-pretreated BM-MSCs significantly improved systolic function. Other echocardiographic parameter did not differ among the groups. There was no difference in the changes in body weight, serum BNP concentration, heart weight, LV systolic pressure, or LV end-diastolic pressure among the groups (Fig. 4). LV dP/dt was significantly improved by candesartan-pretreatment (A-BM vs. BM) with BM-MSCs; however, there was no additional effect of candesartan-pretreatment in the group of candesartan oral administration group (N.S. CNT-A vs. A-BM+A).

In this study, the beneficial effect was observed even in the ARB-pretreated BM-MSC transplantation group. The effect of ARB is known to cause an irreversible biological change in the cell, the "so-called" memory effect; therefore, such memory effect might affect cardiac function in vivo. To check this possibility, we cultured three groups of BM-MSCs: cells with candesartan for 2 weeks (ARB), cells without candesartan (CNT), and cells with candesartan for 1 week followed by 1 week without candesartan (1 week-ARB: washout for 1 week). The GeneChip analysis was performed among them, then the hierarchical clustering was used using the average distance method [20]. The gene expression pattern of 1 week-ARB was similar to CNT; therefore, the effect of ARB on BM-MSCs was reversible from the aspect of gene-chip analysis.

Incidence of Myocardial Transdifferentiation of ARB-Pretreated BM-MSCs In Vivo

To evaluate myocardial transdifferentiation of BM-MSCs in vivo, immunohistochemical analysis was performed. Antibodies against cardiac troponin-I (Trop-I) and connexin 43 were used. Confocal laser microscopic images could not detect EGFP-positive cardiomyocytes having clear striation staining pattern of Trop-I in the BM group. Sometimes enucleated EGFP-positive fragments of the cell at the center of the MI zone were observed, but taking the number of the injected EGFP-positive cells into account, the incidence seemed to be rare, as was reported previously [6, 19]. On the other hand, EGFP-positive and Trop-I double positive cells with clear striation staining pattern were observed at the marginal zone of the MI area in the candesartan-pretreated BM-MSC transplanted group (A-BM, Fig. 5F–5I). The oral

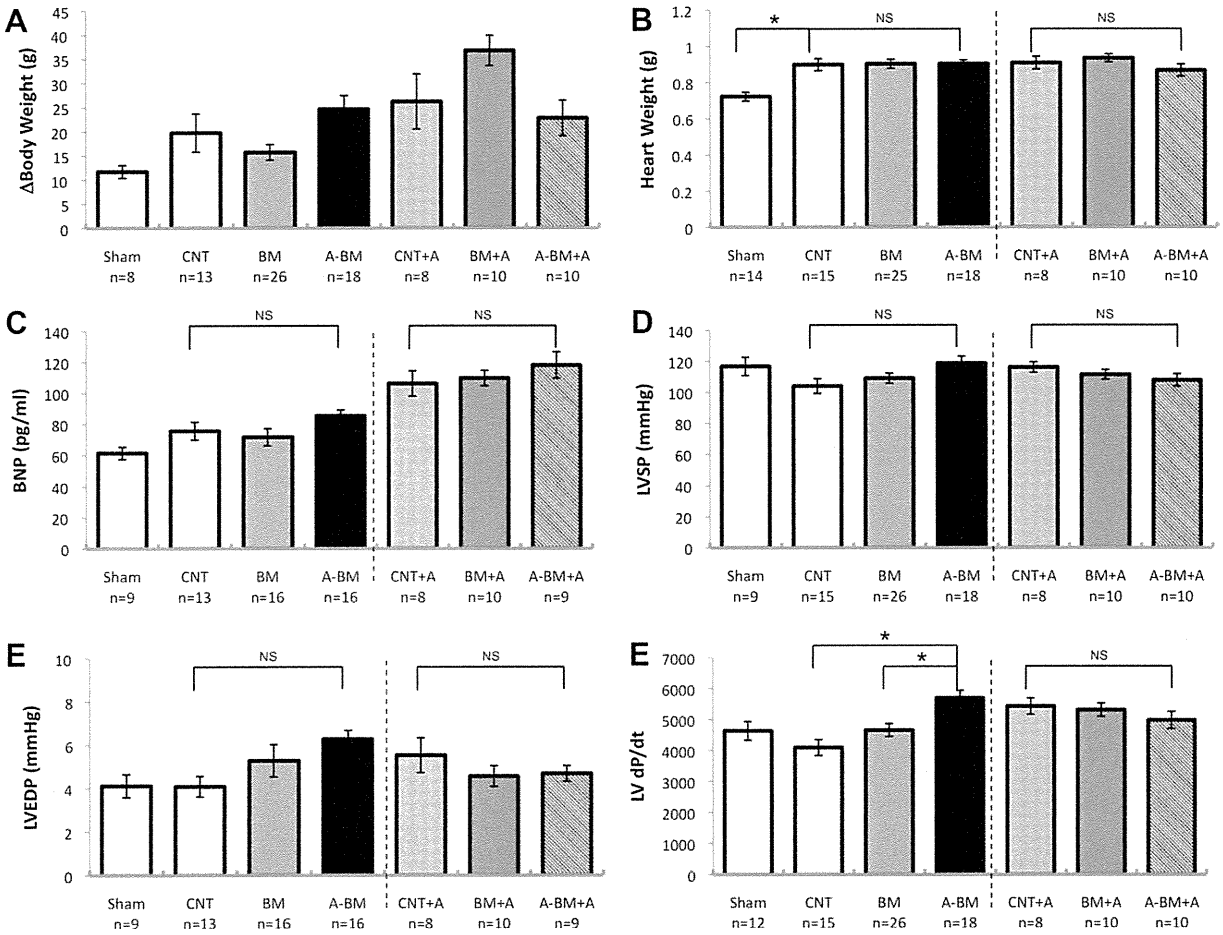

Figure 4. Effect of candesartan-pretreated bone marrow-derived mesenchymal stem cell (BM-MSC) transplantation and/or oral administration of candesartan on body weight, serum BNP concentration, and hemodynamic parameters. There was no difference in **(A)** changes in body weight, **(B)** heart weight, **(C)** BNP concentration, **(D)** left ventricular (LV) end-systolic pressure, or **(E)** end-diastolic pressure. **(D):** Effect of BM-MSCs on LV positive dP/dt is significantly improved by pretreatment with pioglitazone. **(F):** The LV dP/dt was significantly improved by transplantation of candesartan-pretreated BM-MSC (A-BM). *p<0.05. Abbreviations: BM, bone marrow; BNP, brain natriuretic peptide; CNT, control MI; LV, left ventricle; LVEDP, left ventricular end- pressure; LVSP, left ventricular systolic pressure.

administration of candesartan increased the incidence of survival of the EGFP/Trop-I double positive cells in vivo (A-BM+A, Fig. 5A–5E, 5J).

Genesis of Angiogenic Humoral Factors Derived from BM-MSCs by ARB

Angiogenic humoral factors were detected in the supernatant of the culture medium of BM-MSCs, suggesting that they are secreted from BM-MSCs, as reported previously [19]. However, the administration of 3 μmol/l of candesartan did not significantly affect the concentration of these angiogenic factors (Fig. 6). On the other hand, the angiogenic effect of candesartan-pretreated BM-MSCs was observed in vivo (Fig. 7A, 7B). In the peri-MI NZ, a CD34 positive area was not different among CNT, BM, and A-BM groups (without oral administration of candesartan). On the other hand, in the MI area, a CD34 positive area was significantly higher in A-BM group (vs. BM group). Oral administration of candesartan, significantly increased the CD34 area (CNT+A vs. CNT) in the peri-MI normal area and significantly increased it in the MI area. Masson trichrome staining and calculated MI volume at 2 weeks after transplantation (Fig. 7C, 7D) showed significant reduction of MI volume by pretreatment with candesartan of engrafted BM-MSCs (BM vs. A-BM) and the effect of pretreatment was not significantly augmented by the oral administration of candesartan.

Discussion

The Effect of Pretreatment with ARB in Human Neonatal BM-MSCs

The ARB did not affect the morphology of BM-MSCs and did not increase secretion of angiogenic humoral factors from BM-MSCs. The pretreatment with ARB significantly increased the CTE in vitro and in vivo. As pretreatment with ARB was essential for the effect on CTE, we concluded that the effect of ARB is not mediated by murine cultured myocardium, but directly affects BM-MSCs themselves, modifying the character of BM-MSCs. As the effect was not mediated by PD123319 as a selective AT2R blocker, the effect of ARB was mediated by the blockade of AT1R. In our previous article [19], activation of PPAR-γ significantly increased the CTE in BM-MSCs and the effect was completely blocked by GW9662, as a specific blocker of PPAR-γ receptor. The effect of telmisartan, which is known to have the strongest PPAR-γ activation activity among the ARBs, on CTE was partially blocked by GW9662, suggesting that the effect of ARBs is not mediated by PPAR-γ receptor activation activity. The

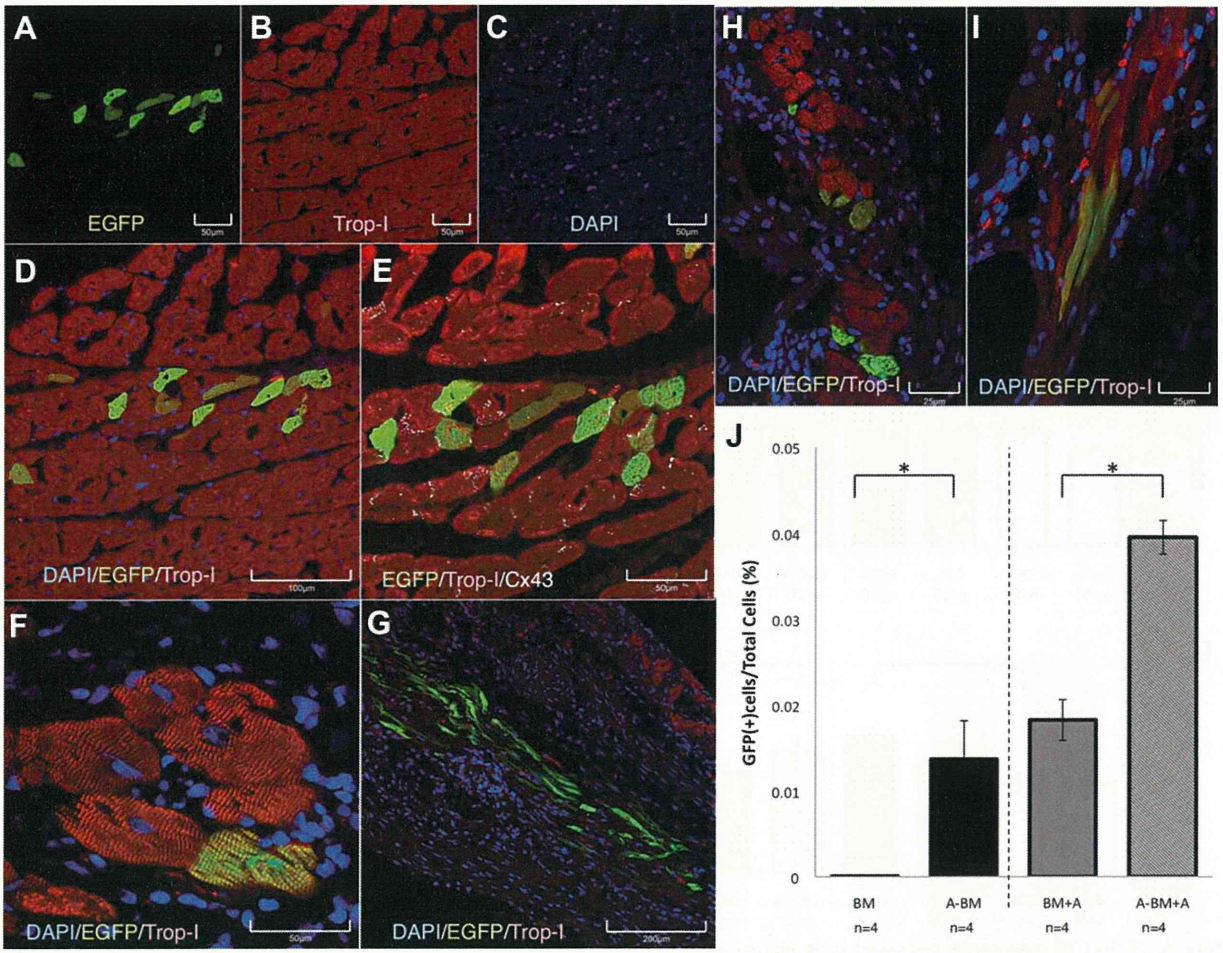

Figure 5. Both pretreatment and oral administration of candesartan significantly improved the incidence of survival of bone marrow-derived mesenchymal stem cell (BM-MSC)-derived cardiomyocytes in vivo. Confocal laser microscopic image of immunohistochemistry using anti-cardiac troponin-I antibody (red; Trop-I) is shown. **(A–C):** Lower magnification view for enhanced green fluorescent protein (EGFP) (green; **A**), Trop-I **(B)**, and 4′-6-diamidino-2-phenylindole (Blue; **E**) is shown. After transplantation of candesartan-pretreated BM-MSCs in the presence of oral administration of candesartan (A-BM+A), EGFP-positive cells can be observed at the margin of the myocardial infarction (MI), but there were many EGFP/Trop-I double positive cardiomyocytes survived at the peri-MI zone **(A)**. **(D):** Higher magnification view of merged image is shown. **(E):** The Trop-I positive cells are surrounded by dot-like staining of connexin 43 (white; Cx43). **(F):** Higher magnification view clearly shows striation staining pattern of Trop-I in the EGFP-positive cells. **(G):** At the center of MI zone (A-BM group), many EGFP-positive cells were enucleated and were negative for Trop-I. **(H, I):** However, there were some EGFP, Trop-I double positive rod-shaped cells at the center of MI zone. **(J):** The percentage of EGFP/Trop-I double positive cells in the injected EGFP-positive cells was averaged and is shown. By pretreatement with candesartan, the rate was significantly improved (A-BM vs. BM), and oral administration of candesartan additionally improved the incidence of EGFP/Trop-I double positive cells in vivo. Scale bars = 50 μm **(A–C, E, F)**, = 100 μm **(D)**, = 200 μm **(G)**, and = 25 μm **(H, I)**, respectively. *$p<0.05$. Abbreviations: BM, bone marrow; DAPI, 4′-6-diamidino-2-phenylindole; EGFP, enhanced green fluorescent protein; GFP, green fluorescent protein; Trop-I, troponin-I.

molecular mechanism of the effect of ARBs on CTE is still unclear. Further experiments should be done.

In the absence of valsartan as an AT1R selective blocker, administration of AT did not affect CTE; however, in the presence of valsartan, AT significantly increased CTE, suggesting that the relative stimulation of AT2R increased CTE. Furthermore, AT in culture medium seems to be generated by ACE activity in BM-MSCs, as the administration of ACE inhibitor to the BM-MSCs in culture significantly increased CTE in vitro. Furthermore, aliskiren did not affect the CTE; therefore, rennin and angiotensinogen did not play a role, but the angiotensin-I in the culture medium or autocrine from BM-MSCs must be a major source for AT.

Mechanism of Improving Systolic Function with ARB

Although EGFP-positive cardiomyocytes were observed in the candesartan-treated BM-MSC transplanted group, the number of them seems to be low for causing improvement in systolic function in vivo, as was seen in this study.

Concordant with the previous in vivo study [8] and clinical study [14], in the absence of BM-MSC transplantation, oral administration of candesartan suppressed the post-MI LV remodeling and progressive worsening of LVEF (CNT vs. CNT+A) at 2 weeks after MI. Furthermore, in this study, even in the absence of oral administration, the beneficial effect was observed in the candesartan-pretreated BM-MSC transplantation group. In this study, the effect of default BM-MSC transplantation was modest and there was no statistical significance from the control MI group. These data suggest that the ARBs modify the biology of BM-MSC, which play an important role in suppressing post-MI LV remodeling. This trend was observed in hemodynamic parameters and histological data. Pretreatment with candesartan significantly improved the efficacy of BM-MSC transplantation in augmentation of LV dP/dt and reduction in MI volume. Such

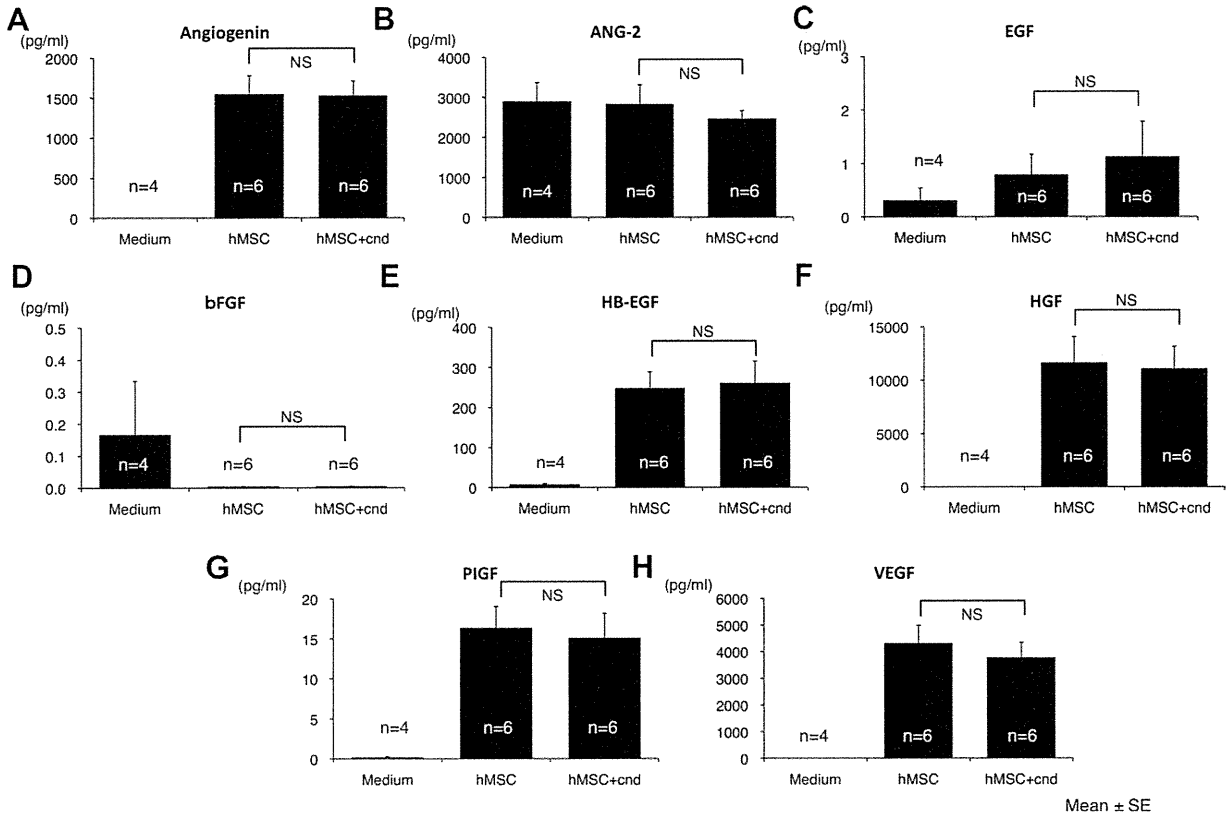

Figure 6. Secretion of angiogenic humoral factors from bone marrow-derived mesenchymal stem cells (BM-MSCs) into the culture medium supernatant and the effect of candesartan in vitro. Concentration of angiogenic humoral factors in **(A)** angiogenin, **(B)** angiotensin-2 (ANG-2), **(C)** epidermal growth factor (EGF), **(D)** basic fibroblast growth factor, **(E)** heparin-binding EGF-like growth factor, **(F)** hepatocyte growth factor, **(G)** phosphatidylinositol-glycan biosynthesis class F protein, and **(H)** vascular endothelial growth factor in culture medium was measured by enzyme-linked immunosorbent assay and averaged. Candesartan (cnd) treatment did not cause any significant change in angiogenic humoral factors secretion from BM-MSCs into the culture medium. Abbreviations: ANG-2, angiotensin-2; bFGF, basic fibroblast growth factor; cnd, candesartan; EGF, epidermal growth factor; HB-EGF, heparin-binding EGF-like growth factor; HGF, hepatocyte growth factor; hMSC, human mesenchymal stem cell; PIGF, phosphatidylinositol-glycan biosynthesis class F protein; VEGF, vascular endothelial growth factor.

cardioprotective effect of ARB-pretreated BM-MSCs may be due to augmentation of angiogenic effect and/or anti-apoptotic paracrine effect of BM-MSCs by pretreatment with ARB. The beneficial effect of ARB-pretreated BM-MSCs was also reported in the ischemia-reperfusion brain injury model [17], in which it was pointed out that both the stimulation of AT2R and blockade of AT1R have a significant effect on reducing brain damage in vivo and this data well correlated with our CTE data in vitro. In this study, the effect can be observed even by BM-MSC transplantation at 2 weeks after MI; therefore, the BM-MSC-induced angiogenesis might have suppressed ongoing post-MI LV remodeling. In this study, there was discrepancy between the angiogenic effect of ARB-pretreatment in BM-MSCs in vitro and in vivo. We speculated that additional angiogenic effect of BM-MSC transplantation by ARB-pretreatment might require graft-host interaction, that is, immunological reaction or inflammation in the host myocardium.

Cell Fusion-Independent Cardiomyogenic Transdifferentiation

Extensive evidence of cell fusion-independent cardiomyogenic transdifferentiation of human MSCs was presented in our previous study [6, 9–11, 19]. In this study, the incidence of cell fusion was approximately 1% and it was not affected by ARB pretreatment; therefore, the increase in EGFP-positive cardiomyocytes by ARB treatment was due to an increase in efficiency of cardiomyogenic transdifferentiation in vitro. Furthermore, there were no EGFP/Trop-I double positive rod shaped cardiomyocytes in the default BM-MSC transplanted group; on the other hand, the appearance of significant numbers of EGFP/Trop-I double positive cardiomyocytes was observed in ARB-pretreated BM-MSC transplanted group. This suggests an improvement of CTE of BM-MSCs in vivo by ARB pretreatment. Taking into account our previous study and our present in vitro experiment, we concluded that our observed EGFP/Trop-I double positive cells in vivo are caused by cardiomyogenic transdifferentiation.

Clinical Application

The efficacy of human BM-MSC transplantation had been modest [14, 15], and a new method for BM-MSC transplantation that will gain dramatic improvement in efficacy is expected. Genetic modification, that is, over-expression of the *AKT*-gene was reported to improve efficacy of BM-MSC transplantation in vivo [21]; however, use of such genetically modified cells raises a safety concern, that is, tumorgenecity. In comparison with the genetic modification, modification of BM-MSCs by ARBs, which are commonly used for heart failure patients, is a method that is ready to use for clinical patients.

In addition to the beneficial efficacy for cardiac function, this experimental model may also give us a clue to improving CTE in vivo, which is very essential for cardiac regenerative therapy. The precise mechanism for cardiomyogenic transdifferentiation of human BM-MSCs has been unclear. As the

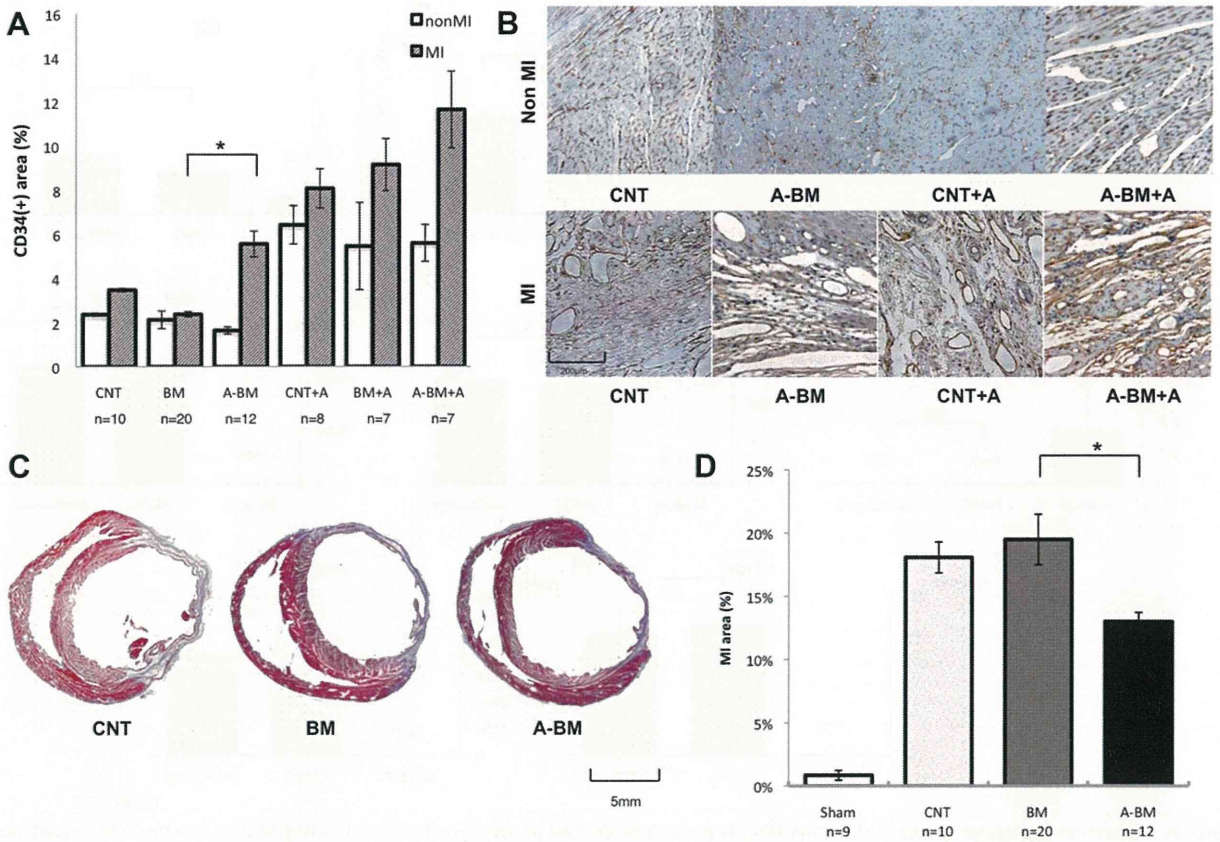

Figure 7. Effect of bone marrow-derived mesenchymal stem cell (BM-MSC) transplantation and/or treatment with candesartan on vessel density and infarction size in the heart in vivo. **(A):** The percentage of CD34 positive area in control myocardial infarction (MI) (CNT), MI with bone candesartan-pretreated BM-MSCs transplantation (BM), candesartan-pretreated BM (A-BM), and additional oral administration of candesartan after the transplantation (CNT+A, BM+A, A-BM+A) are calculated and averaged. **(B):** Representative microscopic image of immunohistochemistry using anti-CD34 antibody to detect vessels at center of MI zone and peri-MI normal zone (non-MI) are shown. Scale bar = 20 μm. Pretreatment with candesartan significantly increased vessel density at MI zone; on the other hand, oral administration of candesartan significantly increased vessel density at non-MI zone. **(C):** Representative masson-trichrom staining of the heart at the tendinous cord level of CNT, BM, and A-BM are shown. The digitized data were measured and calculated in **(D)**. By the candesartan-pretreatment, BM-MSC transplantation significantly decreased in percentage fibrosis volume. Scale bar = 5 mm. *$p<0.05$. Abbreviations: BM, bone marrow; CNT, control; MI, myocardial infarction.

incidence of cardiomyogenic transdifferentiation of human BM-MSCs is extremely rare, it has been impossible to statistically analyze the effect on CTE of various drugs or interventions in vivo. Therefore, there has been no systematic strategy for improvement of CTE of BM-MSCs until our previous article [6, 9–11, 19]. Our in vivo model of ARB-treated BM-MSCs is able to statistically analyze the effects of drugs on CTE, which is important for further improvement of CTE. In vitro, the pioglitazone's effect on CTE was independent from the effect of ARB; therefore, the additional administration of pioglitazone, as a PPAR-γ activator may be expected to improve CTE further. Further experiments should be done.

Study Limitation

In our previous study, we have used BM-MSCs obtained from a 41-year-old and a 90-year-old men. The CTE results were 1% and 0.3% in vitro [19], respectively. In this study, the CTE of default BM-MSCs from neonates was approximately 3%–5%. This data implies BM-MSCs obtained from younger generations that may have higher cardiomyogenic transdifferentiation ability. As ARB is known to have a potential for an anti-aging effect, the effect of ARB on BM-MSCs might increase the CTE by ARB's anti-aging effect on BM-MSCs. Further experiments should be done on this issue.

In vivo MI model was performed by two series (Sham, CNT, BM, A-BM series and CNT-A, BM-A, A-BM-A series) at different periods. As it was difficult to control the size of the MI at the coronary ligation, the size of the MI of later series are slightly larger (N.S.) than the former series. Therefore, we did not perform statistical analysis on some parameters between the series (separated by dotted line in the figures). The serum BNP level and the size of percentage MI volume are slightly larger in the later series. In this study, intra-individual difference values were compared with the values of the two series.

Conclusion

Pretreatment with angiotensin receptor blockers (ARBs) in culture activate human marrow-derived mesenchymal stem cells by angiotensin-II receptor type 1 blockade. ARBs-pretreated human marrow-derived msenchymal stem cells was significantly improved cardiomyogenic transdifferentiation efficiency in vitro and in vivo, and transplantation of the ARBs-pretreated cells significantly improved cardiac function and can be a promising cardiac stem cell source from which to expect cardiomyogenesis.

ACKNOWLEDGMENTS

The research was partially supported by a grant from the Ministry of Education, Science and Culture, Japan. A part of this work was undertaken at the Keio Integrated Medical Research Center.

DISCLOSURE OF POTENTIAL CONFLICTS OF INTEREST

The authors indicate no potential conflicts of interest.

REFERENCES

1 Boheler KR, Czyz J, Tweedie D et al. Differentiation of pluripotent embryonic stem cells into cardiomyocytes. Circ Res 2002;91:189–201.
2 Makino S, Fukuda K, Miyoshi S et al. Cardiomyocytes can be generated from marrow stromal cells in vitro. J Clin Invest 1999;103:697–705.
3 Orlic D, Kajstura J, Chimenti S et al. Bone marrow cells regenerate infarcted myocardium. Nature 2001;410:701–705.
4 Tomita S, Li RK, Weisel RD et al. Autologous transplantation of bone marrow cells improves damaged heart function. Circulation 1999;100:II247–II256.
5 Asahara T, Murohara T, Sullivan A et al. Isolation of putative progenitor endothelial cells for angiogenesis. Science 1997;275:964–967.
6 Tsuji H, Miyoshi S, Ikegami Y et al. Xenografted human amniotic membrane-derived mesenchymal stem cells are immunologically tolerated and transdifferentiated into cardiomyocytes. Circ Res 2010;106:1613–1623.
7 Terai M, Uyama T, Sugiki T et al. Immortalization of human fetal cells: The life span of umbilical cord blood-derived cells can be prolonged without manipulating p16INK4a/RB braking pathway. Mol Biol Cell 2005;16:1491–1499.
8 Takeda Y, Mori T, Imabayashi H et al. Can the life span of human marrow stromal cells be prolonged by bmi-1, E6, E7, and/or telomerase without affecting cardiomyogenic differentiation? J Gene Med 2004;6:833–845.
9 Hida N, Nishiyama N, Miyoshi S et al. Novel cardiac precursor-like cells from human menstrual blood-derived mesenchymal cells. Stem Cells 2008;26:1695–1704.
10 Nishiyama N, Miyoshi S, Hida N et al. The significant cardiomyogenic potential of human umbilical cord blood-derived mesenchymal stem cells in vitro. Stem Cells 2007;25:2017–2024.
11 Okamoto K, Miyoshi S, Toyoda M et al. 'Working' cardiomyocytes exhibiting plateau action potentials from human placenta-derived extraembryonic mesodermal cells. Exp Cell Res 2007;313:2550–2562.
12 Grauss RW, Winter EM, van Tuyn J et al. Mesenchymal stem cells from ischemic heart disease patients improve left ventricular function after acute myocardial infarction. Am J Physiol Heart Circ Physiol 2007;293:H2438–H2447.
13 Hou M, Yang KM, Zhang H et al. Transplantation of mesenchymal stem cells from human bone marrow improves damaged heart function in rats. Int J Cardiol 2007;115:220–228.
14 Chen SL, Fang WW, Ye F et al. Effect on left ventricular function of intracoronary transplantation of autologous bone marrow mesenchymal stem cell in patients with acute myocardial infarction. Am J Cardiol 2004;94:92–95.
15 Hare JM, Traverse JH, Henry TD et al. A randomized, double-blind, placebo-controlled, dose-escalation study of intravenous adult human mesenchymal stem cells (prochymal) after acute myocardial infarction. J Am Coll Cardiol 2009;54:2277–2286.
16 Matsushita K, Wu Y, Okamoto Y et al. Local renin angiotensin expression regulates human mesenchymal stem cell differentiation to adipocytes. Hypertension 2006;48:1095–1102.
17 Iwanami J, Mogi M, Li JM et al. Deletion of angiotensin II type 2 receptor attenuates protective effects of bone marrow stromal cell treatment on ischemia-reperfusion brain injury in mice. Stroke 2008; 39:2554–2559.
18 Ikegami Y, Miyoshi S, Nishiyama N et al. Serum-independent cardiomyogenic transdifferentiation in human endometrium-derived mesenchymal cells. Artif Organs 2010;34:280–288.
19 Shinmura D, Togashi I, Miyoshi S et al. Pretreatment of human mesenchymal stem cells with pioglitazone improved efficiency of cardiomyogenic transdifferentiation and improved cardiac function. Stem Cells 2010 (in press).
20 Kami D, Shiojima I, Makino H et al. Gremlin enhances the determined path to cardiomyogenesis. PLoS One 2008;3:e2407.
21 Gnecchi M, He H, Liang O et al. Paracrine action accounts for marked protection of ischemic heart by Akt-modified mesenchymal stem cells. Nat Med 2005;11:367–368.

See www.StemCells.com for supporting information available online.

RESOURCE

nature biotechnology

Screening ethnically diverse human embryonic stem cells identifies a chromosome 20 minimal amplicon conferring growth advantage

The International Stem Cell Initiative[1]

The International Stem Cell Initiative analyzed 125 human embryonic stem (ES) cell lines and 11 induced pluripotent stem (iPS) cell lines, from 38 laboratories worldwide, for genetic changes occurring during culture. Most lines were analyzed at an early and late passage. Single-nucleotide polymorphism (SNP) analysis revealed that they included representatives of most major ethnic groups. Most lines remained karyotypically normal, but there was a progressive tendency to acquire changes on prolonged culture, commonly affecting chromosomes 1, 12, 17 and 20. DNA methylation patterns changed haphazardly with no link to time in culture. Structural variants, determined from the SNP arrays, also appeared sporadically. No common variants related to culture were observed on chromosomes 1, 12 and 17, but a minimal amplicon in chromosome 20q11.21, including three genes expressed in human ES cells, *ID1*, *BCL2L1 and HM13,* occurred in >20% of the lines. Of these genes, *BCL2L1* is a strong candidate for driving culture adaptation of ES cells.

In human ES cell cultures, somatic mutations that generate a selective advantage, such as a greater propensity for self-renewal, can become fixed over time[1]. This selection may be the reason for the nonrandom genetic changes found in human ES cells maintained for long periods in culture. These changes, mostly detected by karyotypic analyses, commonly involve nonrandom gains of chromosomes 12, 17, 20 and X, or fragments of these chromosomes[2–12]. The embryonal carcinoma (EC) stem cells of human teratocarcinomas, the malignant counterparts of ES cells, though typically highly aneuploid, always contain amplified regions of the short arm of chromosome 12 and, commonly, gains of chromosomes 1, 17 and X[13–16]. Gain of chromosome 20q has also been noted in yolk sac carcinoma and nonseminomatous germ cell tumors, which contain EC cells[17–19]. Such observations suggest that these specific genetic changes in ES cells may be related to the nature of pluripotent stem cells themselves rather than the culture conditions. Mouse ES cells also undergo karyotypic changes upon prolonged passage[20], often with gain of mouse chromosomes 8 and 11 (ref. 21); mouse chromosome 11 is highly syntenic with human chromosome 17 (ref. 22).

Structural variants in otherwise karyotypically normal human ES cells have also been described[10,11,23,24]. These structural variants include gains on chromosome 4, 5, 15, 18 and 20 and losses on chromosome 10, although only gains on chromosome 20 were commonly observed in multiple cell lines.

Marked epigenetic changes have also been noted on prolonged passage; studies of global DNA methylation in human ES cells found considerable instability with time in culture[25,26]. Functional gain of the X chromosome, resulting from loss of X-chromosome inactivation in culture-adapted ES cells with two karyotypically normal X chromosomes has been reported[27]. On the other hand, some imprinted genes retain their monoallelic expression over long-term culture of human ES cells, although this stability is not invariant for all loci[28–31].

Because stem cells can adopt alternative fates (that is, self-renewal, differentiation or death), it might be expected that those maintained in the pluripotent state for many passages would be subject to strong selection favoring variants that enhance the probability of self-renewal[32]. Viewed in this light, the increased frequency of genetic variants in ES cell cultures over time might be considered inevitable[33]. Indeed, ES cell lines do often show progressive 'adaptation' to culture, with the result that late-passage cells may be maintained more easily, showing enhanced plating efficiencies[27]. Similarly, some mouse and human EC cell lines derived from germ cell tumors are nullipotent, as if selected for the capacity for self-renewal exclusively[34,35]. Taken together, these observations suggest that acquisition of extra copies of portions of chromosomes 12, 17, 20 and X by human ES and EC cells is driven by increased dosage of a gene or genes that favor self-renewal, independent of culture conditions.

However, there are also reports of human ES cell lines that have been maintained for many passages *in vitro* without overt karyotypic changes. It has been argued that some culture techniques, such as manual 'cutting and pasting' of ES cell colonies, favor maintenance of cells with a diploid karyotype[3,6]. As the appearance of a genetic variant in an ES cell culture must involve both mutation and selection, the low population size in cultures maintained by these methods may simply beat the mutation frequency[33]. Nevertheless, culture conditions themselves might influence the mutation rate independently of selection, and a population bottleneck, such as cloning, could allow a viable genetic variant to dominate in the absence of a selective advantage.

[1]A full list of authors and affiliations is provided at the end of the paper.

Received 6 September; accepted 26 October; published online 27 November 2011; doi:10.1038/nbt.2051

Candidate genes from the commonly amplified regions can be posited to provide the driving force for selection of variant ES cells, but direct evidence for the involvement of any specific gene is lacking. For example, *NANOG*, on human chromosome 12p, promotes the self-renewal of ES cells when overexpressed[36–38], but one of the two minimal amplicons of chromosome 12p in EC cells has been reported to exclude the *NANOG* locus[39]. It is also unclear to what extent changes affecting different loci are selected independently of one another or whether alterations at some loci act synergistically. Further, overexpression of disparate genes affecting a common pathway(s) could lead to an increased proliferative potential. Although the frequent gain of chromosomes 12, 17, 20 and X in both ES and EC cells argues for a selective advantage independent of culture conditions, changes affecting other regions might be more likely to depend upon culture conditions.

To provide better insight into the frequency and types of genetic changes affecting human ES cells on prolonged passage, the International Stem Cell Initiative (ISCI) surveyed by karyology and high-resolution SNP array 125 independent human ES cell lines, provided by 38 laboratories in 19 countries around the world, particularly to identify the common genetic changes that occur during prolonged culture (**Supplementary Table 1**). An opportunity was also taken to screen the samples against a specialized custom DNA methylation array focused on polycomb-target genes. These likely play a role in controlling ES cell differentiation and could be primary targets for the types of epigenetic change observed in cancer cells[40]. Thus, they may provide a source of selective advantage for variant stem cells. In most cases, each line was analyzed at both an early- and a late-passage level, using all three types of assay. The scale and design of this screen helped ensure that the ES cell lines sampled were representative of the world population. A group of 11 human iPS cell lines from three laboratories was also included to provide a pilot comparison of these pluripotent cells derived by reprogramming. Our results indicate that the common gains of chromosomes 12 and 17 in human ES cells are unlikely to be driven by the gain of single genes, but that the gain of chromosome 20 may be driven by the gain of a single gene, *BCL2L1*.

RESULTS

Diversity and population structure of the cell lines surveyed

To define the range of ethnicity represented by the human ES cell lines included in this study, we first analyzed the SNP calls identified in the SNP array data by referencing them to ethnically defined human genotyping data sets. Of the samples submitted for SNP analysis, three cell lines were included twice, and four pairs of ES cell lines and a set of three lines were identified as having a full sibling relationship (**Supplementary Table 1**). After accounting for these, 112 genetically unrelated ES cell lines passed SNP quality-control criteria. Subsequent analysis allowed us to determine whether specific structural variants found in particular cell lines are limited to the population from which they were derived or common to all human ES cell lines studied.

For population structure analysis, the international breadth of this study required the use of a diverse set of reference samples to compare to these 112 genetically unrelated cell lines. The reference samples were pooled from the HapMap[41], the human genome diversity panel (HGDP)[42] and the Pan-Asian SNP Initiative[43] to generate an ethnically diverse set of 1,868 reference samples. We performed cluster analysis[44] of the human ES cell samples against these reference samples, using the CEU (European), Chinese, Japanese and African HapMap populations as references, to arrive at the population structure of the human ES cell lines analyzed (**Fig. 1a**).

Of the 112 genetically unrelated ES cell lines, 61 (54%) were of European ancestry (excluding Middle East–East European and Central-South Asia–South European), 31 (28%) of Asian ancestry, 3 (3%) of African ancestry, 12 (10%) of Middle East and East European ancestry, and 4 (4%) of Central-South Asian and South European ancestry (**Table 1**). The European ES cell lines were further stratified using a recently described comprehensive European reference set[45] and were found to match subpopulations from many different regions of Europe (**Fig. 1b**). The cell lines of Asian descent were stratified into those of East Asian origin, including those of Han Chinese, Korean, Japanese and Indian origin, and those of Central or Central-South Asian origin (**Fig. 1c,d**). Five of the cell lines classified as Middle East and East European clustered with one another but not particularly close to any of the reference samples used in this study, namely clusters belonging to HGDP-Central/South-Asia, HGDP-Middle East and the HGDP-European samples (**Fig. 1d**). Four of these five lines were derived in Iran, and are most likely of Persian ancestry, a population not represented in the reference samples. It is notable that the nine ES cell lines most commonly cited in the scientific literature are representative of the genetic backgrounds of populations from northern, northwestern and central European, Han Chinese, Indian and Middle Eastern populations (**Table 1**).

Karyotype analysis

Stability of the cell lines. Analyses were carried out on all 120 human ES cell lines (including duplicate and sibling cell lines) provided for karyotyping at both early- and late-passage levels ('paired' lines), as well as on five additional lines that were provided only in early passage (**Supplementary Table 1**). Among this total of 125 lines, 42 (34%) had abnormal karyotypes (defined as at least two metaphases with identical, abnormal karyotypes of at least 30 metaphases screened) in at least one passage level. The data from this study confirm that human ES cells are commonly diploid soon after derivation, and that many do retain a normal karyotype after many passages (**Fig. 2a**).

Late-passage cultures of the paired lines were approximately twice as likely to have a chromosome abnormality (39/120, 33%) as those from the early-passage cultures (17/120, 14%). Among the five lines submitted only at an early-passage level, one (20%) had an abnormal karyotype with an extra copy of chromosome 17q. Of the 39 paired lines with abnormal karyotypes at late passage, 24 were normal at the early passage, whereas the remaining 15 also had abnormalities at both passage levels. In this case, the abnormalities seen at the late passage were mostly similar to those seen at the early passage. About half of all the abnormalities involved combinations of chromosomes 1, 12, 17 and 20 (**Fig. 2a**).

A number of cultures were mosaic with, mostly, two populations of cells, one with a normal karyotype and one with a particular abnormal karyotype; 10 of 24 with abnormalities only at late passage, and 8 out of 15 with abnormalities at both passage levels were mosaic (**Supplementary Table 1**). Five lines that were mosaic at early passage showed an increase in the abnormal cell population at late passage. In all of these cases, the abnormality involved extra copies of chromosomes 1, 12, 17, 20 or X. One pair showed additional chromosome changes in the late passage and one pair had unrelated abnormal karyotypes at each passage level. Two lines were scored as abnormal in early passage but normal at late passage. However, both were mosaic, with 3/30 metaphases in one case with a translocated chromosome t(2:19), and 5/30 metaphases in the other with a duplication on chromosome 13. Both chromosomal rearrangements were unique to these lines and most likely represent random changes that were outcompeted by the normal cells over time.

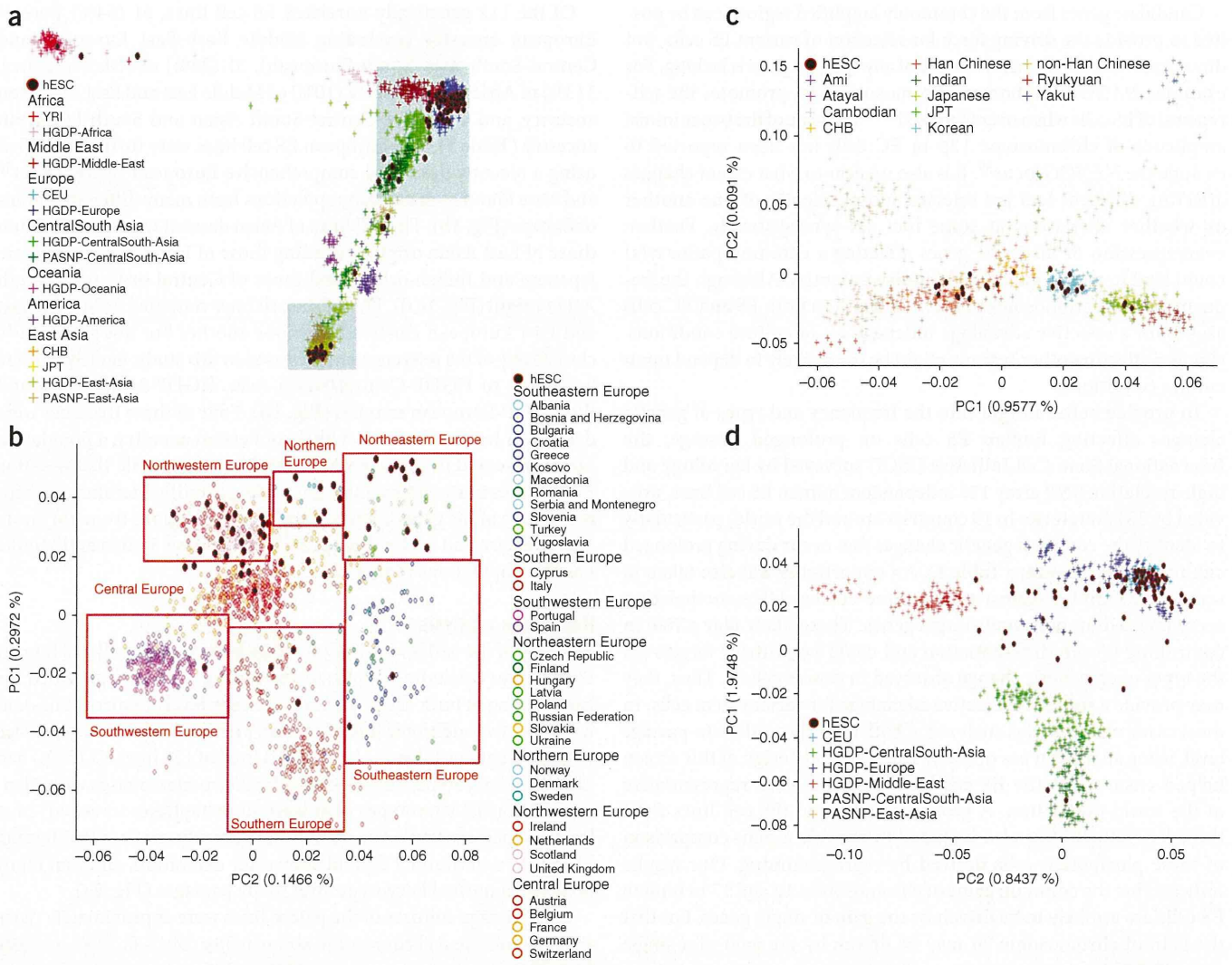

Figure 1 Population structure of the human ES cell lines analyzed. Principal component (PC) analyses were conducted on the entire final merged data set. PC1 and PC2 are plotted on the *y* and *x* axes, respectively. (**a**) The overall distribution of the human ES cell lines studied compared to the major ethnic groups identified in the HapMap study[41], the human genome diversity panel (HGDP)[42] and the Pan-Asian SNP Initiative[43]. (**b**–**d**) The cell lines were further subdivided to show their relationships to European (**b**), East Asian and Indian (**c**) and Middle East-European–Central South Asian populations (**d**).

Among the 11 iPS cell lines examined, three exhibited chromosome abnormalities, a frequency (27%) comparable to that found in ES cell lines. Of these, one line (RR01) exhibited trisomy 12 at both early and late passage. The other two lines were provided only at one passage level; one had a trisomy 12 (RR05) and one an inversion on chromosome 5 (RR03). None of these abnormalities were present in the somatic cells from which they were derived. These results are consistent with recent analysis of human iPS cell chromosomal instability both in the general frequency of aberrations and over-representation of chromosome 12 alterations[12,46].

A common source of cells with abnormal karyotypes. The proportion of cell lines with abnormal karyotypes did increase with delta, the difference in estimated number of population doublings ($P = 0.048$) (**Fig. 2b**). There was also a marked variation in the proportion of abnormal ES cell lines submitted by the different participating laboratories. The 42 abnormal lines were among cell lines submitted by 21 laboratories, whereas no abnormal lines were found among the other 38 lines submitted from the remaining 11 laboratories. This was not directly linked to the delta of the submitted lines and might simply reflect the stochasticity of mutation, or could imply a laboratory effect. The cell lines in each category were from diverse ethnic origins, and were cultured under very similar conditions, although a role for subtle variations in culture technique cannot be excluded. Nevertheless, consistent with suggestions that enzymatic mass-passaging techniques may favor the generation of abnormalities, a twofold higher proportion of the paired lines that had an initially normal karyotype but became abnormal at late passage were passaged by enzymatic methods (18/58, 31%), relative to those passaged by the manual cut-and-paste technique (6/43, 14%) (χ^2, $P = 0.009$). This effect is significant even after adjusting for delta ($P = 0.017$).

Candidate regions/genes. Aberrations of all chromosomes with the exception of chromosome 4 were observed (**Fig. 3**). However, most chromosomes were affected in very few instances, and four cell lines with particularly abnormal karyotypes accounted for many of these sporadic changes (**Supplementary Table 1**). In addition, there were three instances of balanced rearrangements seen as sole aberrations,

Table 1 Ethnic origin of human ES cell lines analyzed indicating ancestry of those most often cited

Ancestry	Number of cell lines[a]	Most commonly used cell lines	No. citations (2008 to 2009)[b]
European	**63 (61[c])**		
Italian	4		
Southwestern European	2		
Southeastern European	2		
Northeastern European	14[d]		
Northern European	8	BG01	13
Northwestern European	24[d]	HUES7	18
Central European	11	H1	95
Asian	**33 (32[c])**		
Central Asian	3		
Central-South Asian	1		
Han Chinese	14	HES2	16
		HES3	14
Japanese	3		
Korean	9		
Indian	3[d]	HES-1	6
African	**4 (3[c])**		
East African	1		
West African	3[d]		
Middle East–East European	**14[e] (12[c])**		
		H9	122
		H7	25
		HSF-6	12
Central-South Asia South European	**4**		
Total cell lines	**118 (112[c])**		

[a]The numbers of cell lines shown includes only those that passed quality control for SNP analysis. [b]UMass Stem Cell Registry (http://www.umassmed.edu/iscr/hESCusage.aspx). [c]Total number of genetically unrelated cell lines. [d]Includes two cell lines from siblings. [e]Includes three cell lines from siblings.

a translocation between 2 and 19 in an early-passage human ES cell culture, an inversion of 11 in a late-passage culture, for which the early passage was normal, and a Robertsonian translocation between chromosome 21 and 22 in both passages of one line. There were also abnormalities affecting chromosome 7 in seven ES cells, but five came from one laboratory, suggesting an unknown cause particularly associated with that group, perhaps related to their derivation of ES cells from prenatal genetic screening material. By contrast, in most abnormal lines (25/42), the changes involved one or more of chromosomes 1, 12, 17 and 20. Of the 17 lines that were abnormal in early passage, eight had abnormalities involving these chromosomes, whereas, of the 24 lines that acquired abnormalities between early and late passage, 16 lines had changes involving acquisition of one or more of these chromosomes (**Fig. 2a**). Among the gains, there were minimal amplicons affecting the telomeric region of chromosome 17 (17q25) in two lines, and another affecting 20q11.2 was apparent in another line (**Fig. 3**). Gains of only the short arm of chromosome 12 were found in three cell lines.

The large differential in frequency between gain and loss of chromosomes is remarkable. In contrast to the 39 ES cell lines that showed gains of chromosomal material in late passage, 20 lines showed losses of chromosomal material. However, only two lines exhibited chromosomal deletions that were not caused by unbalanced translocations (one, UU03, had two unrelated deletions of chromosomes 6 and 18), although even in these there were also unrelated chromosome gains. Excepting the deletions on chromosome 7, which only occurred in the lines from one laboratory, three regions showed recurrent loss, 10p13-pter (five cases), 18q21-qter (five cases) and 22q13-qter (three cases); in several cases these were the sole changes (**Fig. 3**).

Structural changes determined by molecular karyotyping

Identification of ES cell–associated structural variants. As genomic structural changes do occur below the ~5 MB detectable limit of karyotyping, we used SNP data to identify structural variants and detect structural changes down to a minimum of 1 kb in length. We identified structural variants for all samples that passed quality control, but restricted our detailed analyses to those cells judged to have a normal karyotype, because of the difficulty of ascribing functional significance to a small structural genomic change in a background of a much larger karyotypic abnormality. Nevertheless, we did examine the breakpoints in six cases of balanced rearrangements (PP-107, NN-12, J-02, CC-05, AA-03, RR-03) but found no evidence of structural variants associated with these (**Supplementary Table 1**). In addition, although loss of heterozygosity can be detected with the SNP platform, we focused our attention primarily on structural variant analysis as this is the more likely structural change to lead to a selective advantage. Nonetheless, we provide a spreadsheet of overlapping loss of heterozygosity across the 225 human ES cell samples and an associated .bed file with all loss-of-heterozygosity calls (**Supplementary Data Sets 1** and **2**). Structural variants were identified in the 200 DNA samples from karyotypically normal ES cells that passed quality control by comparison with the reference genome (hg18). Further quality controls removed one sample due to an extremely high number of structural variants called and two more for extremely high total length of structural variants (**Supplementary Fig. 1**). A total of 27,409 deletions with an average size of 40.2 kb, and 7,413 duplications with an average size of 95.4 kb, were detected. The sizes of these structural variants and the total number of differences between deletions and duplications are consistent with previous structural variant studies of human populations[47]. As structural variants are a common feature of variation between individuals, the majority of structural variants detected in the human ES cells most likely represent the condition of the genomes of the respective embryos from which they were derived, and are unrelated to human ES cell culture.

To aid in distinguishing culture-associated structural variants, we compared the human ES cell structural variants to those identified using the same platform to analyze a set of 267 HapMap samples (raw data directly supplied by Illumina). Though relatively restricted in population diversity compared to our human ES cell data set, the HapMap samples provide a set of common reference structural variants. Our subsequent analyses focused only on variant regions enriched in human ES cell lines over the HapMap samples. We identified 504 regions of gain and 860 regions of deletion in the karyotypically normal ES cell lines as 'ES cell associated' (**Supplementary Data Set 3** and **Supplementary Table 2**).

Genome-of-origin variants. The apparent ES cell–associated structural variants most likely include some rare and/or localized variants absent in the HapMap set, yet unrelated to human ES cell culture selection. There are a number of examples in which a particular variant occurs in a single line in both the early and late passage. Although we cannot exclude that such variants arose in culture before the early-passage samples being obtained, it is more likely they represent rare and/or localized variants present in the genomes of the donated embryos. We did see such a case among the iPS cell lines for which we have SNP data from the parental somatic cell line. For instance, in three iPS cell lines derived from the same parental fibroblast, the same rare gain (chr12:106,928,902-107,008,902) was detected in both the early and late passages and the parental line (**Supplementary Data Set 3**). Also, among the sibling human ES cells lines, we found recurring rare variants specific to each family. For instance, a gain at chr3:45,220,749-45,263,539 was found in the early and late passages of human ES cell lines G02 and G05, although this allele was absent in G04, the third of these sibling lines. At another

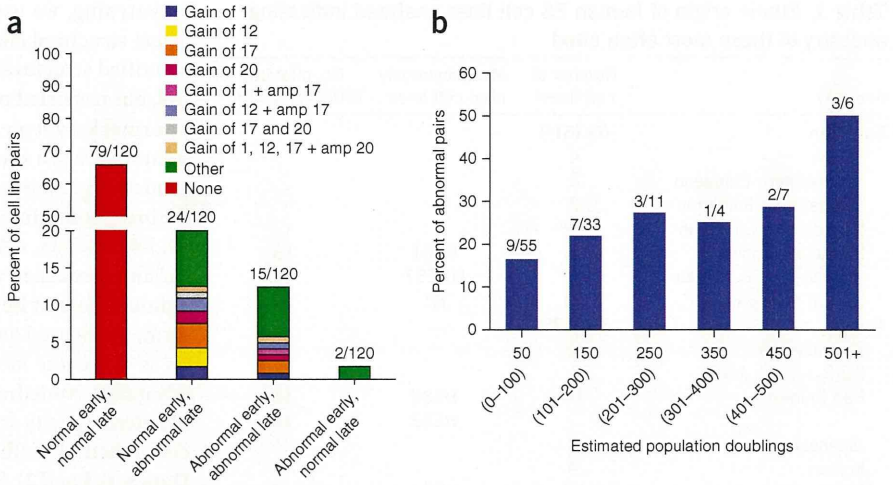

Figure 2 Cytogenetic changes occurring during prolonged passage of human ES cells. (**a**) Percentage of human ES cell line pairs that exhibited a karyotypic abnormality in either early or late passages, or both. Cell lines were excluded if they were known to be derived from karyotypically abnormal embryos. The ES cell pairs are grouped according to whether the chromosome change was observed at late passage only (normal early, abnormal late), both at early and late passages (abnormal early, abnormal late) or early passage only (abnormal early, normal late) and no chromosomal change (normal early, normal late). The percentage of cell lines that have individual gains of chromosomes 1, 12, 17 and 20, gain of chromosomes 1 and 17, or gain of chromosomes 1, 12, 17 and 20 are highlighted. Chromosome changes not involving 1, 12, 17 and 20 are indicated as 'Other'. The numbers above each bar indicate the total number of lines that fall into the four categories out of the total number of pairs of lines analyzed. Two cell lines (CO2 and CC05) in the 'abnormal early, abnormal late' category were known to be derived from karyotypically abnormal embryos (a trisomy 13 and ring chromosome 18). One abnormal cell line (AA06) has been excluded from this figure as only one passage was available for analysis. (**b**) Proportion of pairs of lines that acquired karyotypic abnormalities over different periods in culture. The pairs of lines are grouped according to 'Delta', the difference in estimated population doublings between the early and late passages. Only those lines that had a normal karyotype at the early-passage level were included in the analysis, and of those only 115 pairs could reliably be assigned an estimated population doubling time estimate.

location, chr3:167,536,633-167,837,107, a gain occurs in the early and late passage of all three of these sibling lines. For the purposes of this study, we have assumed that none of these rare variants arose during ES cell culture, and we define them as 'genome-of-origin' variants (**Supplementary Table 2**).

Dynamically changing variants. Some structural variants that were detected are represented in the HapMap population and change dynamically in ES cell culture, suggesting the labile nature of at least some genomic elements. For example, 18 human ES cell lines had a gain at chr17:75,289,455-75,296,305 (**Supplementary Table 2**, labile structural variant), but this was also present in four HapMap samples. Among the human ES cell samples, this structural variant was present in the late but not early passage of four lines, but in five other definitive cases it was present in the early but not late passage. Thus, this represents a dynamically changing variant with no evidence for positive selection in human ES cell culture but provides an example of the labile nature of the human genome.

Structural variants enriched in late-passage cultures. In the subset of structural variants enriched in the ES cells, there was no overall trend toward a gain of total structural variant numbers between early-passage and late-passage samples: that is, there was an increase in the total number in the late passage of some lines, but a decrease in others (**Supplementary Table 2**). Among the particular structural variants that did show increases in several lines in a late passage, a number encompassed regions known to encode genes that may be relevant to human ES cell behavior, but they were isolated instances. For example, a deletion variant spanning the *SOX21* locus, a gene encoding a transcription factor associated with differentiation of human ES cells, was found in one line (UU03-E), and a minimal deleted region at chr4:983425-997875, which spans the promoter and first exon of *FGFRL1*, was present in the late but not early passage of two lines (L03-l, TT20-l). FGFRL1 is expressed in human ES cells and may act as an inhibitory sink for FGF2, which is important for human ES cell maintenance[48]. Late-passage samples of both the MM01 and TT20 lines share a minimal overlapping deletion variant of ~540 bp at chr3:196,472,618-196,473,157. This spans a highly conserved open reading frame (C3orf21) that is expressed in human ES cells but has no known function[48].

Structural variants in karyotypically normal ES cells

We next analyzed structural variants in regions subject to common karyotypic abnormalities. In one region of chromosome 1q, two cell lines (V09 and FF01) in late, but not early, passage, have an overlapping 3.1 MB gain (chr1:199,985,282-203,092,388), which spans *JARID1B*, a polycomb-related gene encoding a histone H3 lysine-4-demethylase[49,50]. On chromosome 12, two cell lines (B02 and F04) have an overlapping gain of 1.1 MB in chr12:5,592,150-6,749,326 in the late-passage samples. This structural variant is within a minimal amplicon identified by karyology (12p13.31) and includes *NANOG*, *CD9* and *GAPDH*, all of which are expressed in human ES cells. There was little evidence for repeated occurrence of gains below the resolution of standard banding techniques in regions of chromosome 17 (**Supplementary Fig. 2**).

In contrast, there was a striking occurrence of a structural variant gain within chromosome 20 in 22 karyotypically normal cell lines. Notably, these gains, many validated by quantitative PCR (**Supplementary Fig. 3**), are within the minimal amplicon 20q11.2 found by karyology (**Fig. 4**). Among these 22 cell lines, there were five instances where the gain was detected in both early and late passage but 17 instances where it was detected only in the late passage. There were no instances of this gain in early passage but absence in late passage of the same cell line. This gain was also present in an ES cell line (J01) that had an abnormal karyotype at late passage and in an iPS cell line (RR01) that contained an extra copy of chromosome 12 (**Supplementary Table 1**). This strongly suggests that once genomic rearrangements occur in this region, they provide a positive selective advantage during subsequent culture. The least difference in passage number between the early and late passage from the same cell line, which had the gain in the late passage alone, was 22. The apparent strong positive selection for gain of this region suggests that a gene providing a cell-autonomous functional advantage under normal human ES cell culture conditions is encoded within the DNA of the

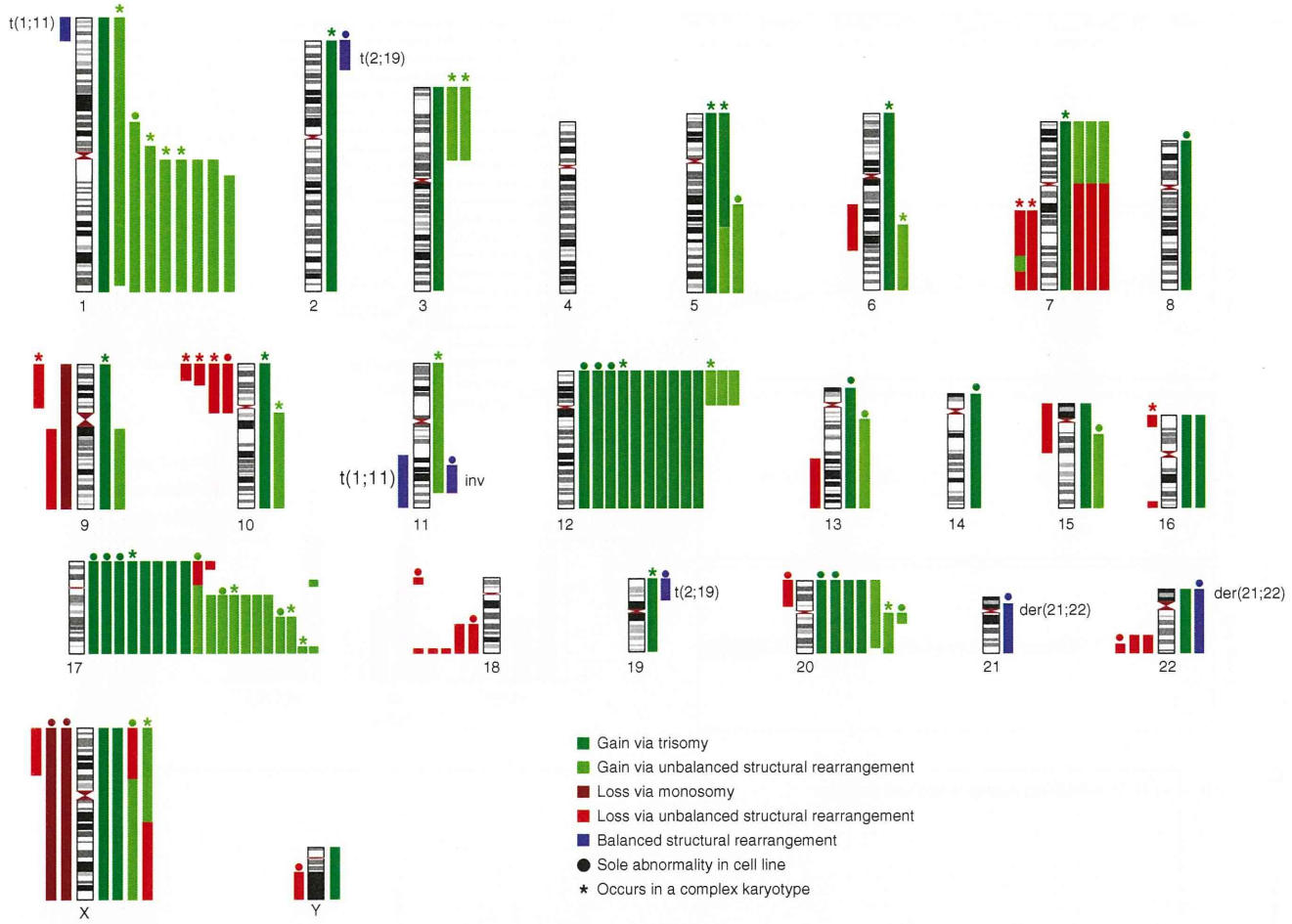

Figure 3 Ideogram demonstrating the chromosome changes found in this study. Each colored bar represents one chromosome change occurrence in one cell line. Chromosome losses and gains are shown to the left and right of the ideogram, respectively, except that those instances where a single chromosome rearrangement results in a gain and a loss the colored bars are shown together for clarity. The cytogenetic changes are color coded: Maroon, loss of a whole chromosome (monopsony); red, loss via a structural chromosome rearrangement (unbalanced translocation or interstitial deletion); dark green, gain of a whole chromosome (trisomy); light green is gain via a structural chromosome rearrangement (unbalanced translocation or interstitial duplication); blue represents the occurrence of an apparently balanced rearrangement the nature of which is labeled. Instances in which a change affected only a single chromosome are denoted by ●, whereas changes associated with complex karyotypes (>5 unrelated chromosome aberrations) are denoted by ★. Two cell lines (C02 and CC05) were known to be derived from karyotypically abnormal embryos and contain a trisomy 13 and ring chromosome 18 respectively. iPS cell lines are excluded from this figure. Based upon these studies the minimal critical chromosomal regions subject to gain in culture adapted human ES cell lines were 1q21-qter, 12p11-pter, 17q21.3-qter and 20q11.2. The minimal regions subject to loss were 10p13-pter, 18q21-qter and 22q13-qter.

shared overlapping region. Moreover, three cell lines (F-01, Q-02 and K-05) that had a normal karyotype and a 20q11.21 structural variant gain in early passage acquired an abnormal banded karyotype in samples from later passage. The late-passage abnormal karyotypes of F-01, Q-02 and K-05 were 46,XX,der(15)t(15;17)(p11;q21); (47,XX,+der(1)(t(1;1)(p?21.2;q11); and 47,XX,t(1;11)(p?36;q13),trp(17)(p11.2),+20, respectively. This preliminary evidence suggests that early gains in 20q11.21 might promote further subsequent genetic change.

The duplicated regions of chromosome 20 in the various cell lines and the minimal amplicon are diagrammed in **Figure 4b**. The proximal ends of each of the structural variant gains within chromosome 20 are presumed to lie in a nonbridged sequencing gap sized at 1 MB near the centromeric region of the long arm. The most proximal SNP identified in all these gains is the first occurring after this gap, at position 29,267,954. The distal end of the gain varies across the lines. The longest gain extends to 31,793,485 with a measured length of 2.5 MB, similar to the shortest karyotypically identified gain in this region, dup(20)q11.21 in cell line UU01 (**Fig. 3**). The shortest gain is 0.55 MB extending to 29,821,940 and contains 13 genes (**Fig. 4c**). Three of these genes, *ID1*, *BCL2L1* and *HM13*, are known to be expressed in human ES cells based on mRNA-Seq data (**Fig. 4c**) and published microarray data[27]. Although a single RefSeq-annotated microRNA lies in this region, there is no evidence for its expression in human ES cells[51]. Further, combined with the mRNA-Seq data, ChIP-Seq data from H1 human ES cells of histone modifications, considered universal predictors of enhancer and promoter activity (H3K4me3, H3K27ac), do not suggest additional functional regions other than those associated with the three RefSeq genes identified as expressed in human ES cells (**Fig. 4c**).

When four pairs of cell lines with and without the chromosome 20 gain were analyzed, there was no clear correlation between increased expression and the presence of the 20q11.21 gain for these three expressed genes (**Fig. 4d**). Nevertheless, preliminary results indicated a strong selective advantage in culture for cells with the gain

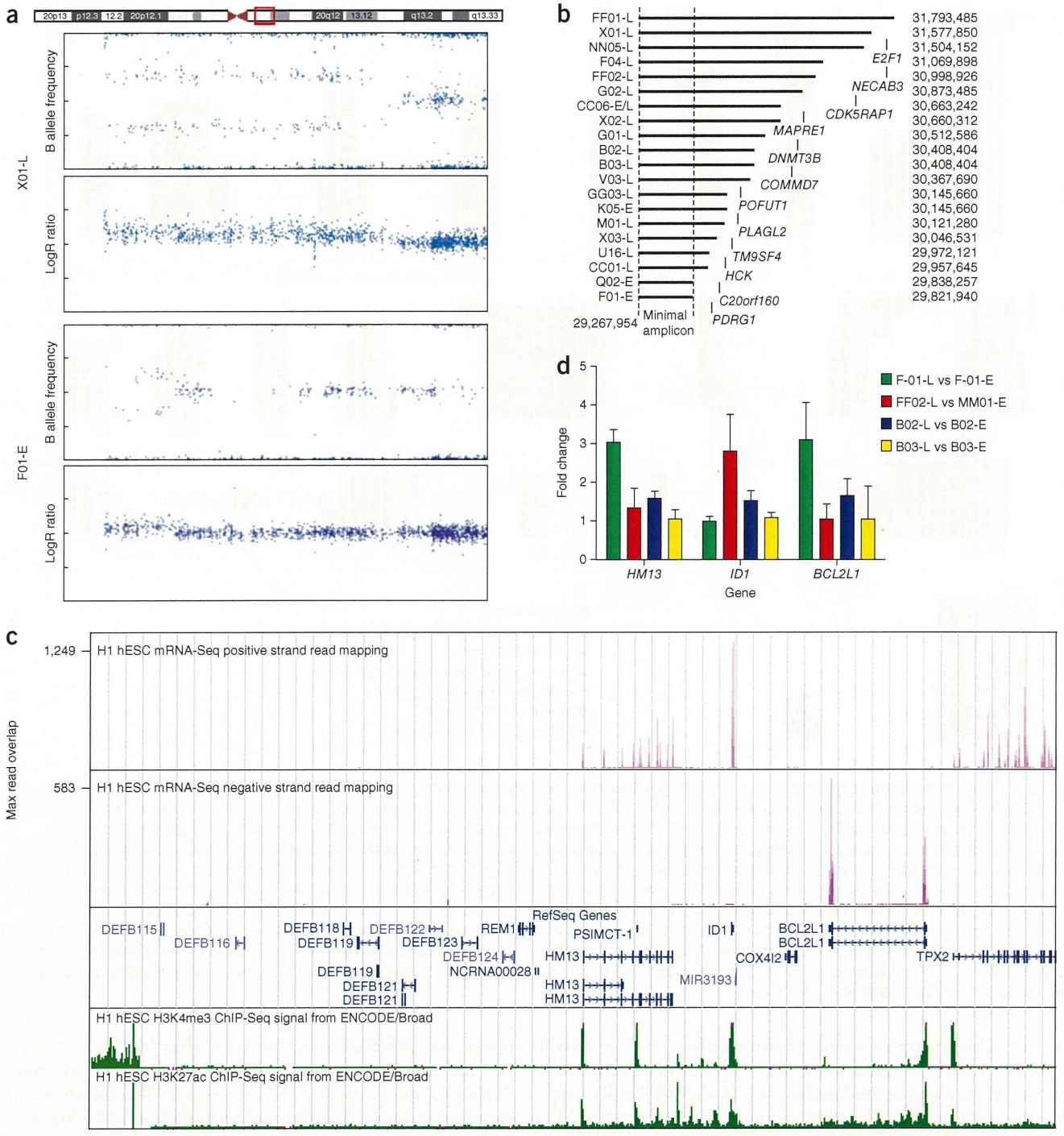

Figure 4 Copy number variation occurrence in human ES cell lines during prolonged passage. (**a**) 20q11.21 gain. The region on chromosome 20 frequently found to experience gain over extended human ES cell culture is indicated by the red boxed region in the chromosome ideogram. Also shown are the B allele frequency and logR ratio plots representing instances of one of the longest and one of the shortest 20q11.21 structural variants. (**b**) Length representation of all individual occurrences of gains in the 20q11.21 region. Samples from which the structural variant was derived are indicated on the left-hand column. The invariant 5′ region and the variable 3′ positions are indicated. Position of genes outside of the minimal amplicon that show greater than 20 RPKM level of expression in human ES cells are shown (RPKM = number of reads that map per kilobase of exon model per million mapped reads for each gene). (**c**) Expression, RefSeq gene, and regulation tracks in the minimal amplicon. Positive and negative strand mRNA-Seq data from H1 human ES cells indicating polyA RNA transcripts expressed within the minimal amplicon region (chr20:29,267,954-29,853,264) are shown together with H1 human ES cell ChIP-Seq data of histone modifications considered universal predictors of enhancer and promoter activity. (**d**) Comparison of expression levels of three genes (*HM13*, *ID1*, *BCL2L1*) contained within the identified minimal 20q11.2 amplicon between early- (normal) and late-passage (20q11.2 CNV carrying) samples. MM01 and FF02 are genetically identical sub-lines from two separate laboratories, MM01 has no amplification at 20q11.2, whereas FF02 possesses a copy number change at 20q11.2 that includes the identified minimal amplicon (**b**).

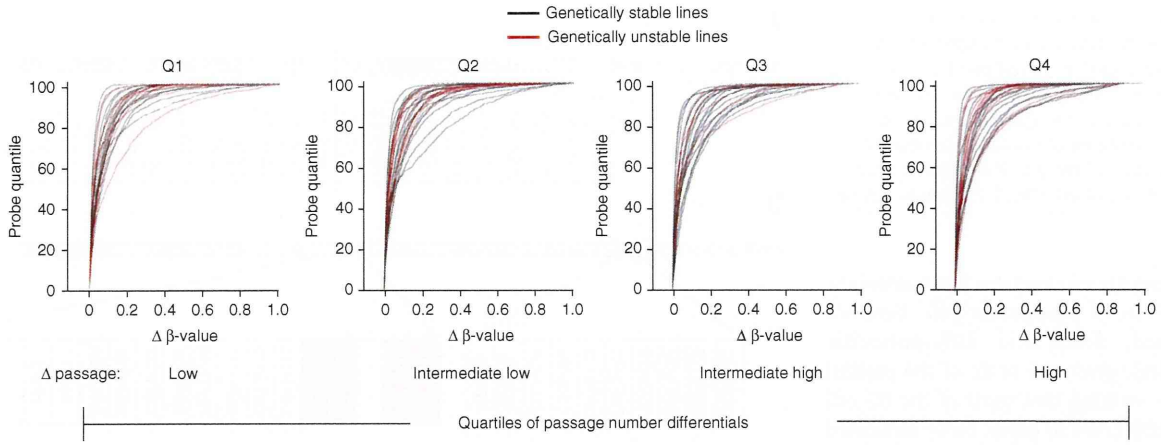

Figure 5 Cumulative distribution function of methylation changes in human ES cells in this study. The change in DNA methylation is represented by empirical CDF curves of the absolute difference in DNA methylation between early- and late-passage cell-line pairs for all 1,536 analyzed probes. The black curves denote genetically stable lines; the red curves denote genetically unstable lines. All analyzed lines were divided into quartiles based on the passage-number difference between the early and late member of each pair. The first quartile contains the lines with the lowest difference in passage number between the early and late sample (range 4 to 47), whereas the fourth quartile contains the lines with the highest difference in estimated population doublings (range 210 to 1,482).

over those without (**Supplementary Fig. 4**). It has also been recently reported that Bcl-X_L, the long, anti-apoptotic isoform encoded by the *BCL2L1* locus, can suppress apoptosis in human ES cells and increase their cloning efficiency[52]. Further, when we transfected MM01 ES cells with a constitutive vector encoding Bcl-X_L, the predominant isoform expressed in human ES cells, these cells showed a distinct growth advantage with respect to the parental cells (**Supplementary Fig. 4**).

DNA methylation analysis

To examine whether cell lines that are genetically unstable at the karyotype level tend to show higher levels of epigenetic instability, we analyzed DNA methylation patterns, focusing on developmentally relevant genes known to be targets of abnormal promoter DNA methylation in cancer[40], and thus most likely to be subjected to selection for altered expression during culture adaptation. For this we used a custom GoldenGate DNA methylation array developed to interrogate DNA methylation changes in known polycomb group protein (PcG) targets in human ES cells[53]. In general, the DNA methylation patterns of the human ES cells tended to be unstable, with both increases or decreases depending upon the locus (**Fig. 5** and **Supplementary Data Set 4**). **Table 2** summarizes those genes that were most frequently subject to gain or loss of methylation during passage, or that showed the least change. Overall, we did not observe any hot spots for DNA methylation at the ~1,500 loci interrogated in the array used in this study, and chromosomes 12, 17 and 20 were not any more methylated, on average, than the rest of the genome.

Table 2 The top 20 genes that were most frequently gained, lost or showed no change in DNA methylation levels in the 120 ES cell lines analyzed at early and late passage

Gained DNA methylation	Lost DNA methylation	No change in DNA methylation
GPC3	*CBLN4*	*NR4A3*
RAB9B	*HIST1H3C*	*EPHA4*
TCEAL4	*LY6H*	*COL12A1*
IL1RAPL2	*HIST1H4L*	*TIGD3*
ESX1	*ANKRD20B*	*SNX7*
TCEAL3	*HIST1H4F*	*PIP5K1B*
AMMECR1	*DMRT2*	*KCNJ2*
MGC39900	*TTLL7*	*T*
LRCH2	*FOXD4L1*	*ZBTB7A*
ZCCHC12	*FOXD4L2*	*IL20RA*
REPS2	*ONECUT1*	*GNAO1*
SOX3	*MAL*	*EPB41L4A*
RP13-360B22.2	*SYT6*	*VDR*
TSC22D3	*BHLHB4*	*HS6ST3*
NHS	*HIST1H3I*	*VGLL2*
TCEAL7	*XTP7*	*SIX1*
MGC4825	*NEUROG1*	*SFT2D2*
GPR50	*TFAP2D*	*BCAN*
BCL2L10	*DRD5*	*ELMOD1*
CDX4	*ASCL2*	*PTGER4*

GPC3 gained more than 5% DNA methylation (range: 98–5%) in over 70% of the samples analyzed, whereas *CBLN4* lost more than 5% DNA methylation (range: 70–5%) in over 60% of them. The genes listed in the "No change" column showed fluctuations in DNA methylation <1% in all samples profiled.

As shown by cumulative distribution function (CDF) curves, most cell lines underwent extensive DNA methylation changes during their time in culture (Online Methods). However, there was a marked difference between the cell lines. For example, in some cell lines there were few changes observed even if there was a large difference in passage level between the early- and late-passage samples (**Fig. 5** Q4 and **Supplementary Table 3**), whereas with other pairs there were large differences observed even when the passage-level difference between the samples was small (**Fig. 5** Q1 and **Supplementary Table 3**). However, the causes of the variation in methylation stability between the lines were not evident. There was no obvious laboratory effect, and the karyotypically abnormal cell lines were not any more unstable than their karyotypically normal counterparts. This suggests that genetic instability played little to no role in the epigenetic instability of the cell lines analyzed. In addition, the DNA methylation patterns of the sibling ES cell lines were as different between themselves as they were between unrelated lines (**Supplementary Data Set 4**), suggesting that the genetic background of human ES cells plays a minor role in the degree of their epigenetic instability.

DISCUSSION

The occurrence of genetic and epigenetic change in human ES cells on prolonged passage is clearly important with respect to their use in regenerative medicine. Understanding the key genes involved and the mechanisms that drive change is important, not only for minimizing the impact of such variants in applications of ES and iPS cells, but also

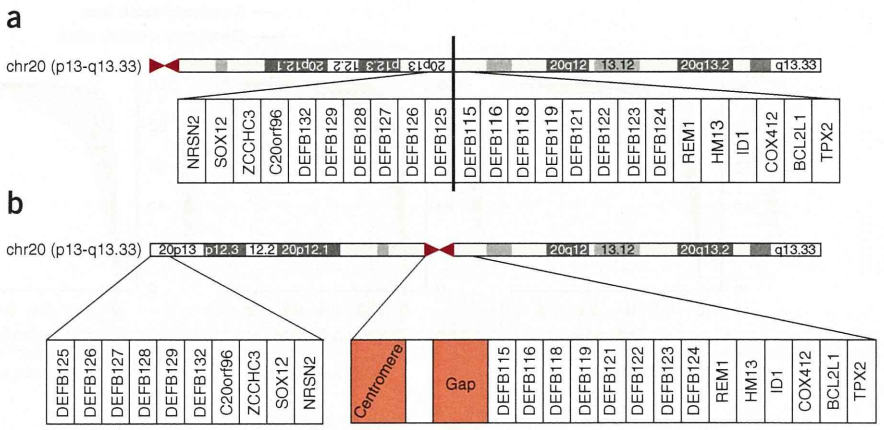

Figure 6 Recent pericentric inversion associated with 20q11.21 susceptibility to gain. (**a**) The ancestral condition of chromosome 20 before a pericentric inversion in the last common ancestor of the gorilla, chimp and human. (**b**) Structure of human chromosome 20 with the location of the gap indicated in which the proximal end of all 20q11.21 amplicons lie.

for exploring the mechanisms that control the fate decisions of pluripotent cells between self-renewal, death and differentiation. Nevertheless, given the scale of the present study, it is striking that most of the ES cell lines studied (79/120 pairs, 66%) remained karyotypically normal, even after many passages, whereas it was only with respect to chromosome 20 that evidence for structural variants in a specific region offering a strong selective advantage could be deduced. Among the small number of iPS cell samples studied, 3 out of 11 had abnormal karyotypes, with 1 of the 3 having the 20q11 gain in the late-passage sample.

Since the first reports of nonrandom chromosomal gain in human ES cells, many studies by standard karyology and by various molecular techniques, including CGH and SNP arrays, have found that, indeed, certain regions of the genome of both ES and, more recently, iPS cells are particularly subject to such genetic change upon prolonged passage in culture. Recently, it was also shown that iPS cells acquire mutations during their derivation, although many such mutations are lost on subsequent passaging[54]. It is commonly assumed that those genetic changes that repeatedly appear in pluripotent stem cells provide variant cells with a growth advantage, but the nature of the selective advantage is unclear. At the molecular karyotype level, it is difficult to disentangle changes that simply reflect variants existing in the human population from those acquired during culture. To address this, we explicitly sought to compare the genomes of a large set of human ES cell lines at two different passage levels and from as diverse a set as possible of the principal laboratories isolating these cells around the world. Although the number of human ES cell lines that have been derived worldwide is uncertain, the 125 ES cell lines analyzed in this study represent a substantial proportion of those commonly available. Notably, our data show that these lines include representatives of most major ethnic groups, reflecting far greater ethnic diversity than previously reported[55,56].

One feature of the human genome emphasized by the current study is that some regions are especially dynamic, particularly but not exclusively those including repetitive elements. In the current panel of ES cells, many regions showed gains or losses between the passage levels, but with no consistency, suggesting that there is no common selection pressure driving the copy number changes. That such dynamically variable regions were readily detected suggests that human ES cell cultures may go through population size restrictions more often than appreciated. Indeed, the cell cycle time of human ES cells is about 18–20 h, but common culture practice involves splitting cultures at low split ratios every 4–5 d or longer. This implies a very large proportion of undifferentiated cells, maybe as many as 90%, are lost between passages of stock cultures[33].

Likewise, the DNA methylation status of the ES cell lines also appeared to change dynamically. Although there was a marked increase in differential DNA methylation with time, indicated by the greater number of DNA methylation changes in the cell lines with the highest differences in passage number, there was also a substantial variation between lines that had undergone similar differences in passage numbers. Thus, human ES cells change not only genetically, but also epigenetically in culture. This conclusion is consistent with several other smaller scale studies that have interrogated human ES cells with respect to either general DNA methylation[25], or imprinting[29,31]. These studies all found DNA methylation and imprinting changes that appeared to be variable between lines and were locus dependent. However, we could not identify specific recurring regions subject to methylation in the genome and there was no observed correlation between DNA methylation changes and chromosomal abnormalities. This suggests that, in general, changes in DNA methylation may be a dynamic process and not necessarily associated with adaptation as such. This point is reinforced by the observation that DNA methylation is markedly different between sibling lines.

In addition to these apparently stochastic and dynamic changes in the genome and epigenome, we did detect marked nonrandom changes in certain parts of the genome. The karyotypic changes seen in the current study match well with other published reports (**Supplementary Fig. 5**)[1]. Gains of chromosomes 1, 12, 17 and 20 and losses of chromosomes 10p and 18q are common in both data sets, and it is only gains of chromosomes 12, 17 and 20 that are often seen as a sole karyotypic change. However, recurrent deletion of chromosome 22q is a novel finding. On the other hand, the gain of chromosome X is a relatively common finding in published studies, whereas only two instances of gain and three instances of loss were observed in the present study. In the light of their relatively frequent occurrence, the minimal amplicons 1q21-qter, 12p11-pter, 17q25-qter and 20q11.2, and perhaps minimal deletions 10p13-pter, 18q21-qter and 22q13-qter deserve special attention as being likely to harbor genes of particular importance for the culture adaptation of human ES cells.

The frequent nonrandom gain of chromosomes 1, 12, 17 and 20 suggests that these chromosomes include a gene(s) that, when overexpressed, confers a growth advantage. Yet, it is striking that in our current extensive study, as in previous studies, structural variant analysis did not point to any frequent repetitive minimal amplicon occurring on chromosomes 1, 12 and 17. Obvious candidate genes are located on these chromosomes—for example, *NANOG* on chromosome 12—but none seems to be more subject to structural variants than other genes on these chromosomes in the absence of karyotypic change. We did see gains spanning the neighboring *SLC2A3/NANOGP1* region described in a recent study[46] but this is just as prevalent, if not more so, within our reference samples and spread across most major ethnic groups, suggesting it is a common structural variant in the human population rather than specific to human ES cells. Together, these observations suggest that the selective advantage attributable to the

gain of chromosomes 1, 12 and 17 may depend upon overexpression of genes or genetic elements at multiple, spatially separated loci, or upon the combination of a structural gene with a long range *cis*-acting regulatory element such that both units must be amplified together to yield an increased function. Alternatively, the appearance of gains within smaller regions may be restricted by chromosomal structure less susceptible to this form of mutation.

By contrast, and in agreement with other studies[5,10,11,23,46,57], our karyotypic and structural variant data point to a region (20q11.21) that, when amplified, apparently drives selection. In this study, because of the much larger number of cell lines and our ability to compare early and late passage, we were able to map the gain to a specific region. Other studies have also reported that gains in this region are associated with enhanced growth characteristics[23], and at least some of the lines in the present study were reported by their contributors to have increased population growth rates (data not shown). The frequency of this gain (25% of the karyotypically normal cell lines), combined with the enrichment in late-passage samples, clearly indicates its selective advantage in human ES cell culture. The mechanism for the selective advantage presumably lies in the minimal region shared by all 22 affected lines, a region containing 13 genes, only three of which are known to be expressed in human ES cells: *HM13*, *ID1* and *BCL2L1*.

A recent genome-wide RNA interference (RNAi) screen highlights the functional importance of *BCL2L1*, an anti-apoptotic factor, in human ES cell biology[58]. This RNAi screen ranked *BCL2L1* twenty-second of 21,121 genes in reducing proliferation after knockdown, whereas *HM13* and *ID1* were ranked 6,679th and 4,224th, respectively[58]. Additionally, a recent structural variant screen of >3,000 specimens from two dozen cancer cell types similarly identified a reoccurring gain on 20q11.21 in which *BCL2L1* was also contained within the minimal amplicon, and knockdown experiments indicated a role for *BCL2L1* in cancer cell proliferation[59]. Recently, it has also been reported that overexpression of the related anti-apoptotic gene, *BCL2*, enhances the survival of human ES cells[60], although *BCL2* is encoded with the region of chromosome 18 subject to recurrent loss in the current data set. Taken together, these observations suggest that similar mutations shared between ES and cancer cells lead to a selective advantage during clonal evolution. The temporal component of our study, where we see[17] instances of early/normal to late/mutated transitions, provides additional support for the notion that the 20q11.21 mutation is the driver mutation in the clonal evolution of these adapted stem cells. Although a role for *ID1* (ref. 61) and *HM13* cannot be excluded, enhanced cell survival due to elevated expression levels of *BCL2L1* offers the most likely mechanism.

The repeated appearance of a structural variant across multiple lines requires both a selective advantage for the variant (e.g., increased expression of *BCL2L1*), and a predisposition for the respective mutation to occur. It is noteworthy that the proximal end of all human ES cell 20q11.21 gains lies within a gap region of the current human assembly[62]. The presumption is that the highly repetitive sequence within this gap predisposes the region to structural rearrangement. With the link between genome rearrangements, primate evolution and disease association[63], it is notable that this gap coincides with a recent chromosomal rearrangement, a pericentric inversion[64], occurring in the last common ancestor of gorilla, chimp and human (**Fig. 6**). The gap region, possibly a centromeric remnant of a tandem duplication[62], introduces the repetitive sequence creating 20q11.21 rearrangement (or amplification) susceptibility. The frequency of appearance that is created by this combination of mutability and the decreased apoptosis warrants routine surveillance similar to that now done in karyotypic analysis.

The identification of genes that drive both cancer progression of EC cells in germ cell tumors and the progressive culture adaptation of ES cells has been a goal since the first clear recognition that gain of sections of the short arm of chromosome 12 is an invariant feature of EC cells[14]. The commonality of the changes in the tumors and in the ES cell in culture suggests common underlying mechanisms. However, the identification of a specific driver gene on chromosomes 1, 12 and 17 has been elusive, suggesting that more than one gene may be involved in the growth advantage of the aneuploid cells. Our present results now point to a specific gene subject to gain, most likely the anti-apoptotic gene, *BCL2L1*, on chromosome 20, that may promote the survival of ES cells *in vitro* and EC cells *in vivo*, thereby providing a strong growth advantage, whether in cancers or *in vitro*.

METHODS

Methods and any associated references are available in the online version of the paper at http://www.nature.com/naturebiotechnology/.

Note: Supplementary information is available on the Nature Biotechnology website.

ACKNOWLEDGMENTS

The International Stem Cell Initiative is funded by The International Stem Cell Forum. The authors would like to acknowledge the following: Medical Research Council, UK (P.W.A., H.M.); Mohammad Pakzad & Adeleh Taei, Royan Institute (H.B., G.H.S.); California Institute for Regenerative Medicine (CIRM) (E.C., P.W.L.); Institute of Medical Biology, A*STAR, Singapore (J.M.C.); Ministry of Education, Youth and Sports of the Czech Republic (P.D., A.H.); Stem Cell Research Center of the 21st Century Frontier Research Program, Ministry of Education, Science & Technology, Republic of Korea (SC-1140) (D.R.L., S.K.O.); Ministry of Science and Technology of China (863 program 2006AA02A102) (L.G.); Swedish Research Council, Cellartis (O.H.); Department of Biotechnology, Government of India, UK-India Education and Research Initiative and the Jawaharlal Nehru Centre for Advanced Scientific Research, Bangalore, India (M.I.); Program for Promotion of Fundamental Studies in Health Sciences of the National Institute of Biomedical Innovation, Leading Project of the Ministry of Education, Culture, Sports, Science and Technology (MEXT), Funding Program for World-Leading Innovative R&D on Science and Technology (FIRST Program) of the Japan Society for the Promotion of Science (JSPS), Grants in-Aid for Scientific Research of JSPS and MEXT (T.I., S.Y., K.T.); Swiss National Science Foundation (grant no. 4046-114410) (M.J.); Shanghai Science and Technology Developmental Foundation (06DJ14001), Chinese Ministry of Science and Technology (2007CB948004) (Y.J.); funding from the North West Science Fund, UK (S.K.); One North East Regional Developmental Agency, Medical Research Council, UK, Newcastle University (M.L.); research funding from the Australian Stem Cell Centre (A.L.L.); The Netherlands Proteomics Consortium grant T4-3 (C.M.); Stem Cell Network, Canada (A.N.); National BioResource Project, MEXT, Japan (N.N.); Singapore Stem Cell Consortium (SSCC) & the Agency for Science Technology and Research (A*STAR) (S.K.W.O., P.R.) and the Genome Institute of Singapore Core Genotyping Lab (P.R.); Academy of Finland, Sigrid Juselius Foundation (T.O.); Conselho Nacional de Desenvolvimento Científico e Tecnológico/Departamento de Ciência e Tecnologia do Ministério da Saúde (CNPq/MS/DECIT), and Fundação de Amparo à Pesquisa do Estado de São Paulo (FAPESP) (L.V.P.); supported by the kind donation of Judy and Sidney Swartz (B.R.); financial support from the Faculty of Medicine, University of New South Wales (UNSW) and the National Health and Medical Research Council (NHMRC) Program Grant no. 568969 (Perminder Sachdev), South Eastern Sydney and Illawarra Area Health Service (SEIAHS) for making hES cell line Endeavour-2 available for this study, and H. Chung and J. Kim for their help in preparing the samples (K.S.); Academy of Finland (grant 218050), the Competitive Research Funding of the Tampere University Hospital (grant 9F217) (H. Skottman).

AUTHOR CONTRIBUTIONS

Project coordination: P.W.A. **Cytogenetic analyses**: D.B., A.D., E.M., K.D.M. and T.G.-L. **Molecular karyotyping by SNP BeadChip**: P.R. **DNA methylation arrays**: R.M.B. and P.W.L. **Administration and data curation**: A. Ford and P.J.G. **Data analysis and manuscript drafting**: P.W.A., S.A., D.B., N.B., R.M.B., P.J.G., K.H., L.H., B.B.K., Y. Mayshar, S.K.W.O., M.F.P. and P.R. **The scientific management of the ISCI project was provided by a steering committee comprising:** P.W.A., N.B., B.B.K., S.K.W.O., M.F.P., J.R. and G.N.S. **Sample contribution**: A. Colman, A. Robins, A. Hampl, A. Bosman, A.M. Fraga, A. Nagy, A.B.H. Choo, A.L. Laslett, A. Feki, A. Kuliev, A. Kresentia Irwanto, B. Reubinoff, B. Sun, C. Denning,